



Identification and robust control methods using ellipsoidal parametric uncertainty descriptions
by Steven Michael Hietpas

A thesis submitted in partial fulfillment of the requirements for the degree of Doctor of Philosophy in
Electrical Engineering
Montana State University
© Copyright by Steven Michael Hietpas (1994)

Abstract:

This dissertation addresses the areas of identification and robust control of uncertain systems. The first portion of this dissertation concerns system identification. The focus of system identification is grounded in the signal analysis technique developed by G. R. B. Prony in 1795. This approach uses two separate least-squares solutions, with the first least-squares solution resulting in the eigenvalues of the output signal and the second yielding the output residues. Previous system identification methods based on Prony signal analysis apply to systems utilizing a continuous-time input. This research develops a method that allows for a sampled-and-held version of the previously used continuous-time input. The new method results in a more simplified algorithm due to the nature of sampled-and-held input signals. Various examples are provided to show the characteristics of the method. The second portion of this dissertation concerns control of systems which are modeled through system identification techniques that provide models with a parametric uncertainty set. The robust control strategy is viewed from dynamic game theory such that a saddle point solution is desired. The game theory method employed has two players: the first player, the feedback control signal, minimizes an energy cost function; and the second player: the set of uncertain parameters, maximizes an energy cost function. It is shown that the optimal control signal necessarily is derived from Linear Quadratic Regulation (LQR) theory. The maximization is performed on the final cost function from the LQR solution and is constrained by an ellipsoidal parameter bound and an appropriate Lyapunov equation. Iterative algorithms for both continuous-time and discrete-time systems are developed. A sufficient condition for the existence of the maximization portion of the discrete-time algorithm is given. Examples show the fixed-point solution of the algorithm is a saddle point. A closed-loop discrete controlled servo-mechanism problem uses the Optimal Volume Ellipsoid (OVE) algorithm of Man-Fung Cheung (1990) for identification of a model and an ellipsoid uncertainty region. The discrete minimax algorithm is applied to determine the optimal state-feedback gain. The servo example is stable and shows the worst-case tracking for the noisy, uncertain system and is compared to the known system.

IDENTIFICATION AND ROBUST CONTROL METHODS USING
ELLIPSOIDAL PARAMETRIC UNCERTAINTY DESCRIPTIONS

by

Steven Michael Hietpas

A thesis submitted in partial fulfillment
of the requirements for the degree

of

Doctor of Philosophy

in

Electrical Engineering

MONTANA STATE UNIVERSITY
Bozeman, Montana

July 1994

D378
H5335

APPROVAL

of a thesis submitted by

Steven Michael Hietpas

This thesis has been read by each member of the thesis committee and has been found to be satisfactory regarding content, English usage, format, citations, bibliographic style, and consistency, and is ready for submission to the College of Graduate Studies.

7/14/94
Date

Donald A. Pierre
Donald A. Pierre
Chairperson, Graduate Committee

Approved for the Major Department

7/14/94
Date

Victor Gerez
Victor Gerez
Head, Electrical Engineering

Approved for the College of Graduate Studies

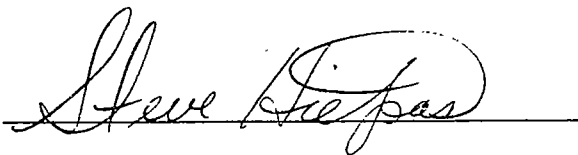
7/23/94
Date

Robert Brown
Robert Brown
Graduate Dean

STATEMENT OF PERMISSION TO USE

In presenting this thesis in partial fulfillment for a doctoral degree at Montana State University, I agree that the Library shall make it available to borrowers under rules of the Library. I further agree that copying of this thesis is allowable only for scholarly purposes, consistent with "fair use" as prescribed in the U. S. Copyright Law. Requests for extensive copying or reproduction of this thesis should be referred to University Microfilms International, 300 North Zeeb Road, Ann Arbor, Michigan 48106, to whom I have granted "the exclusive right to reproduce and distribute my dissertation for sale in and from microform or electronic format, along with the right to reproduce and distribute my abstract in any format in whole or in part."

Signature



Date

7-14-94

ACKNOWLEDGEMENTS

This research was made possible through financial support from the National Science Foundation, the Montana Electric Power Research Association and the Engineering Experiment Station of Montana State University. I express my gratitude to Professor Donald Pierre, my principal advisor, for his continuous support, and certainly for his enduring patience. Dr. Pierre has given me a great example of a professional educator and researcher. Through the efforts of Professor Roy Johnson in his continual quest for upgrading existing computer equipment to the best possible – I had it very nice. Dr. Ming Lau of Sandia Laboratories, New Mexico, played a strong part in the robust control portion of this research, and offered much of his time to the review of earlier work and carefully steered me in the correct direction at crucial times. To the rest of my committee, Dr. James Smith, Dr. Hashem Nehrir, Dr. Curtis Vogel and Dr. Richard Swanson, thank you for the time you spent listening to my concerns and offering advice where needed. I extend my appreciation to all of my fellow graduate students, Cesar Amicarella, Fereshteh Fatehi, Don Hammerstrom, Ed Ray, Tia Sharpe and Stott Woods, who have always shown confidence in me when things were not going as well as I desired. A special thanks to Don Hammerstrom, a great engineer and a good friend, for all the helpful discussions, assistance in mastering L^AT_EX, and for all the exciting racquet ball games. My pastors, Blake Updike and Dave Green, were always available to listen and offer their wisdom and advice when I needed it most. Of course, without a doubt, I thank my parents, Jerry and JoAnne Hietpas, and Jack and Mary Gay Wells for their encouragement. I am fortunate to have wonderful in-laws who also encouraged me throughout this dissertation; thanks

Lance and Marlys Johnson and Collin. I also have the best brother, Tom and sisters, Elise and Tara, who have always been there for me, thanks. My special buddies, Taylor and Aaron, you have always been and always will be an inspiration and joy to me. In addition to these wonderful boys, on June 16, 1994, I was blessed with a beautiful girl, Megan Lynn. Lastly, and most importantly, to my wife Tara, your unfailing love, commitment and confidence in me has kept me going. I owe much of this work to you; thank you so much for being at my side through everything while taking care of the home front. At the beginning of this dissertation, Tara gave me the following quote, Philippians 4:13, New International Version of the Holy Bible; and I close, acknowledging that Christ Jesus is truly the sustainer of all things on this earth.

I can do everything through Him who gives me strength.

TABLE OF CONTENTS

	Page
LIST OF TABLES	ix
LIST OF FIGURES	x
ABSTRACT	xi
1. INTRODUCTION	1
2. DISCRETE PRONY IDENTIFICATION	11
Review of System Identification Methods	11
Autoregressive Models (ARX)	13
State-Space Models	15
Prony Signal Identification for Discrete Control Systems	24
Introduction: Discrete Prony	24
System Characterization	25
Prony Based Analysis	29
Examples	36
Discussion of Results	50
3. SET-MEMBERSHIP APPROACH TO CONTROL DESIGN	54
Ellipsoid Set Estimation	56
Disturbance/Noise Induced Ellipsoid	56
Non-parametric Uncertainty Induced Ellipsoid	58
Linear Quadratic Regulator	62
Continuous-Time LQR	62
Discrete-Time LQR	64
Minimaximization Problems	65
Example: Lau	66
Example: Mills	67
Proposed Minimaximization Problems	68
Discussion of Results	71

TABLE OF CONTENTS — Continued

	Page
4. MINIMAXIMIZATION FOR SINGLE-INPUT SINGLE-OUTPUT SYSTEMS	73
Continuous-Time System Problem Statement	73
Some Useful Results from LQR Control Theory	75
Iterative Solution Approaches	76
Examples	81
Discrete-Time System Problem Statement	87
Iterative Solution Approach	89
On The Nature Of The Solution Of Algorithm 3	90
Set-membership Control Problem	94
Discussion of Results	100
5. CONCLUSION	102
6. FUTURE RESEARCH	106
REFERENCES CITED	109
APPENDICES	117
APPENDIX A - Identification Code	118
runcomp.m	119
id_plt.m	130
diff_model.m	134
diff_modes.m	136
diff_nn.m	140
diff_noise.m	141
pr1.m	145
pr1b.m	153
pr2.m	156
pr2b.m	163
pr3.m	171
prony_in.m	179
u_prony.m	181
get_prony_in.m	183
in_exmpl.m	186
rm_mode.m	187

TABLE OF CONTENTS — Continued

	Page
xdisp_mode.m	189
make_obsvble.m	190
obsv.m	194
sys2obsv_can.m	195
moon1.m	199
moon2.m	203
moon_in.m	206
u_moonen.m	208
get_moon_in.m	209
u_modes.m	211
sysm6.m	212
discr.m	215
fftst.m	217
dir_stamp.m	219
file_stamp.m	220
time.m	222
Chapter 2, Example 4: Equations and Code	223
sys_infty.m	227
rk.m	237
APPENDIX B – Robust Control Code	239
mmJ.m	240
minJ1.m	245
maxJ1.m	246
gradJ1.m	247
maxJ2.m	249
gradJ2.m	250
ricc.m	252
servo.m	254
mmJd.m	263
maxJd.m	271
ove.m	274

LIST OF TABLES

Table		Page
1	Actual system model data for Examples 1-3.	38
2	Input drive data for Examples 1-2.	38
3	Data from Prony algorithm for Example 1.	39
4	Input drive data for <i>discrete Prony</i> of Example 3.	44
5	Example 3 error data for noise applied at $d(t)$	47
6	Final model for Example 4.	49
7	Interval bounds on parameters of Example 1 using OVE algorithm.	98
8	Machine data for Example 4 of Chapter 2.	224

LIST OF FIGURES

Figure,	Page
1 System and actual model in parallel form.	26
2 The linear mass/spring diagram for Examples 1-3.	37
3 Probing input $u(t)$ and its Fourier transform equivalent for Examples 1-2.	38
4 Error in dB for each additional mode set for Example 1.	40
5 The output for both actual, $y(t)$ and model, $\hat{y}(t)$ for Example 1.	40
6 Error in dB for each additional mode set for Example 2.	41
7 The output for both actual, $y(t)$ and model, $\hat{y}(t)$ for Example 2 with additive output noise.	42
8 The output for both actual, $y(t)$ and model, $\hat{y}(t)$ for Example 2 with additive output noise removed.	42
9 The poles of the s -domain for the actual system and the model for Example 2.	43
10 Probing input $u(t)$ and its Fourier transform equivalent for Example 3 using the <i>discrete Prony</i> algorithm.	44
11 Probing input $u(t)$ and its Fourier transform equivalent for Example 3 using the <i>Moonen</i> algorithm.	45
12 The singular values of the Hankel matrix for Example 3 using the <i>Moonen</i> algorithm, no noise case.	46
13 The singular values of the Hankel matrix for Example 3 using the <i>Moonen</i> algorithm with 50dB output SNR.	47
14 One-machine/infinite-bus power system diagram.	48
15 Residue ordering for example 4.	49
16 Detailed diagram of control scheme for Example 4.	50
17 Transient simulation of example 4: Open loop vs. LQG.	51
18 Set-membership adaptive control scheme diagram.	55
19 Illustration of saddle point on the boundary of Ω for Example 1.	84
20 Illustration in two dimension of saddle point condition for Example 1.	85
21 Illustration of saddle point on the boundary of Ω for Example 2.	87
22 LQR costs for plants within interior of uncertainty region using $K^* = 1.4692$; Example 2.	88
23 Set-membership adaptive control detailed block diagram.	97
24 Servomechanism problem for standard LQG and set-membership control.	99
25 Steady-state vector diagram of bus voltages.	224

ABSTRACT

This dissertation addresses the areas of identification and robust control of uncertain systems. The first portion of this dissertation concerns system identification. The focus of system identification is grounded in the signal analysis technique developed by G. R. B. Prony in 1795. This approach uses two separate least-squares solutions, with the first least-squares solution resulting in the eigenvalues of the output signal and the second yielding the output residues. Previous system identification methods based on Prony signal analysis apply to systems utilizing a continuous-time input. This research develops a method that allows for a sampled-and-held version of the previously used continuous-time input. The new method results in a more simplified algorithm due to the nature of sampled-and-held input signals. Various examples are provided to show the characteristics of the method. The second portion of this dissertation concerns control of systems which are modeled through system identification techniques that provide models with a parametric uncertainty set. The robust control strategy is viewed from dynamic game theory such that a saddle point solution is desired. The game theory method employed has two players: the first player, the feedback control signal, minimizes an energy cost function; and the second player: the set of uncertain parameters, maximizes an energy cost function. It is shown that the optimal control signal necessarily is derived from Linear Quadratic Regulation (LQR) theory. The maximization is performed on the *final cost function* from the LQR solution and is constrained by an ellipsoidal parameter bound and an appropriate Lyapunov equation. Iterative algorithms for both continuous-time and discrete-time systems are developed. A sufficient condition for the existence of the maximization portion of the discrete-time algorithm is given. Examples show the fixed-point solution of the algorithm is a saddle point. A closed-loop discrete controlled servo-mechanism problem uses the Optimal Volume Ellipsoid (OVE) algorithm of Man-Fung Cheung (1990) for identification of a model and an ellipsoid uncertainty region. The discrete minimax algorithm is applied to determine the optimal state-feedback gain. The servo example is stable and shows the worst-case tracking for the noisy, uncertain system and is compared to the known system.

CHAPTER 1

INTRODUCTION

Very often, a dynamical system is sufficiently complex such that linear or nonlinear sets of equations that adequately describe the system are not available. This is true for many systems, including sophisticated aircraft, chemical processes, large power systems, etc. Under these circumstances it may be necessary to assume a particular parameterized model and apply system identification techniques to arrive at a useful mathematical model of the system to be controlled. The subject of this dissertation addresses system identification and robust control of uncertain systems.

System identification deals with the problem of building mathematical models of dynamical systems based on observed data from the system. A system is an object in which variables of different kinds interact and produce observable signals. Observable signals that emanate from the system are often referred to as outputs. External signals that can be manipulated by the observer and applied to the system are called controlled inputs. Other system input signals are called disturbances, some of which can be directly measured, while others can only be observed through their influence on the output. Systems such as aircraft, space structures, bridges, ships and power grids, to name a few, are considered dynamical, which means that the current outputs depend not only on the current inputs but also on their earlier values. Outputs of dynamical systems whose external stimuli are not observed, e.g., the sound of a human voice generated by the vibration of the vocal chords, are often called *time series*. This term is common in economic applications. Clearly, the list of examples of dynamical systems can be very long and it stretches over many fields of human endeavor.

A major part of the engineering field deals with how to make good designs based on mathematical models. A model describes the relationship among system variables in terms of mathematical expressions like difference or differential equations. Such models are called *mathematical* (or *analytical*) *models*. Mathematical models may be further characterized by a number of adjectives: time continuous or time discrete, lumped or distributed, deterministic or stochastic, linear or nonlinear, single or multi-input/output, etc. When input and output signals from a system that are subjected to data analysis in order to infer a model, the activity is known as *system identification*.

The construction of a model from data involves three basic entities [1]:

I. The data.

II. A set of candidate models.

III. A rule by which candidate models can be assessed using the data.

The data record should be selected to be maximally informative, subject to constraints that may be at hand. Obtaining maximally informative input-output data is affected by which output signals are measured, when and how the signals are measured, and the choice of input signals for external stimuli. The set of candidate models to choose from is certainly the most important step of the identification procedure. It is here where prior knowledge, engineering intuition and insight have to be combined with the formal properties of models. After selection of an appropriate model one is faced with various methods of fitting the model to the data. One approach to the assessment of the model quality is based on how the model performs when it attempts to reproduce the measured data.

The first part of this dissertation is concerned with system identification. The focus of system identification in this research is grounded in the signal analysis tech-

nique developed by G. R. B. Prony [2] in 1795. In this work, Prony proposed a basic signal analysis method to approximate a signal $y(t)$ by a summation of n weighted exponentials, i.e.,

$$y(t) \approx \hat{y}(t) = \sum_{i=1}^n B_i e^{\lambda_i t}$$

for continuous time $t \geq 0$, where $B_i \in \mathbb{C}$. The approach uses two separate least-squares solutions, each of order n , with the first least-squares solution resulting in the eigenvalues of the signal $\{\lambda_i\}$, and the second yielding the weighting terms (or output residues) $\{B_i\}$. The basic Prony method is a signal analysis method rather than a system identification method. Extending this signal analysis method of Prony to system identification was possibly first presented by Poggio, et al., [3] in 1978. The system input in [3] is a summation of two real exponential inputs.

Typically the number of eigenvalues (or poles) n is chosen sufficiently large (greater than the 'actual' number of eigenvalues) prior to the formulation of the first least-square problem. The problem of solving the first set of equations is equivalent to a linear prediction (LP) problem. Kumaresan and Tufts [4]-[7] address the effect of noise on the solution to the LP problem in the first least-squares formulation. Their work shows, that from the over-determinization (i.e., large n), the effect of using a truncated singular value decomposition (SVD) essentially increases the signal-to-noise-ratio (SNR) in the data prior to obtaining the solution. The sample variance of the parameter estimates are compared to the Cramér-Rao (CR) bound for the pole damping factors and pole frequencies. A description of the Cramér-Rao bound can be found in [1, pages 183-187] and is briefly described here. Suppose we are interested in estimating a set of parameters θ from a set of data denoted by y^N . Let the estimated set be defined as $\hat{\theta}(y^N)$ and the "true value" of θ be denoted by θ_0 . The quality of the estimator can be assessed by its mean-square error matrix:

$$P = \mathbb{E}[\hat{\theta}(y^N) - \theta_0][\hat{\theta}(y^N) - \theta_0]^T$$

where \mathbb{E} evaluates the mean. We may be interested in selecting estimators that make P small. It is then interesting to note that there is a lower limit to the values of P that can be obtained with the various unbiased estimators. Let the probability density function of y^N be given by $f_y(\theta_0; y^N)$ and assumed to be known. The definition of the *Cramér-Rao inequality* is stated as follows:

Definition 1.1 (Cramér-Rao inequality) *Let $\hat{\theta}(y^N)$ be an estimator of θ such that $\mathbb{E}\hat{\theta}(y^N) = \theta_0$ and suppose that y^N may take values in a subset of \mathbb{R}^N , whose boundary does not depend on θ_0 . Then*

$$\mathbb{E}[\hat{\theta}(y^N) - \theta_0][\hat{\theta}(y^N) - \theta_0]^T \geq M^{-1}$$

where

$$M = \mathbb{E} \left[\frac{d}{d\theta} \log f_y(\theta; y^N) \right] \left[\frac{d}{d\theta} \log f_y(\theta; y^N) \right]^T \Bigg|_{\theta=\theta_0} = -\mathbb{E} \frac{d^2}{d\theta^2} \log f_y(\theta; y^N) \Bigg|_{\theta=\theta_0}$$

The matrix M is known as the *Fisher information matrix* and evaluation requires the knowledge of θ_0 , so the exact value of M may not be available to the user. More information on the Cramér-Rao bound when dealing with dynamical systems can be found in [1, pages 186-187].

Further analysis of the effect of the truncated SVD and the variance of the parameter estimates is given in [8] and references therein. Although much of the work in [4]-[7] deals with signal analysis aspects, a transfer function identification example is given in [7]. In this example, however, the input is an impulse signal and after the poles of the system are determined using Prony's method, the zeros of the transfer function (roots of the numerator polynomial) are found using Shank's method [9]. Further investigation of Prony's method for signal modeling of noisy data and model order selection can be found in [10]-[12]. Parameter estimation of exponentially damped sinusoids using higher order statistics (HOS) utilizing Prony's method is explored in [13].

The work in [14]- [20] progressively extends the flexibility of using Prony analysis to perform system identification. In [14] and [15] the input is restricted to be a single square-wave pulse. This approach was improved in [16] where the input is allowed to exhibit a series of step changes, with the input characterized by a single real eigenvalue between step changes. In [17], using an input similar to [16], it is shown that nonzero initial conditions can be identified in addition to the system transfer function. For the results in [14] through [17], the assumed system is not allowed to have a feedthrough term, and the system input is not allowed to have an eigenvalue that is identical to an eigenvalue of the system. Feedthrough terms are included in [18] and [19], however, and in [19] the assumed conditions are relaxed to allow the system to have an eigenvalue that is identical to the one associated with the input. In [20] the class of allowed input signals is expanded: the signals can exhibit jump discontinuities and can be characterized by a finite number of eigenvalues between discontinuities. The advantage of this more general input form is that it can be tailored to excite system modes in frequency ranges of interest. A point in common with several of the later methods mentioned above is that all input signals are required to be time-continuous during each interval of discontinuity, which does not lend well to systems that are microprocessor controlled. This research addresses this point and results in a method that allows for a sampled-and-held version of the general input of [20]. The method developed here provides a more simplified algorithm than that of [20] as a result of the sampled-and-held input.

While there are a large number of identification methods available in the literature; only a few methods of system identification techniques are reviewed in Chapter 2. Following this review of system identification techniques the method based on Prony signal analysis is developed for a discrete controlled system. Once the method is developed, several examples are provided to show various attributes

of the method. Further analysis is provided by comparing the Prony based method to another technique based on a signal energy analysis method that utilizes singular value decomposition. While the method that utilizes SVD for signal decomposition is easier to implement than Prony, there are fewer 'knobs' available for the user to work with in arriving at an optimal model. From an engineering perspective, it is often possible, that the more 'knobs' there are available to use, the better the chance to obtain an acceptable solution. Under the noisiest conditions the Prony method performs slightly better than the SVD method. As a last example, *discrete Prony* identification is applied to a one-machine infinite-bus power system to obtain a low-order model. Linear quadratic control synthesis based on this model is used for transient damping while the system experiences a transmission line fault. The control based on the *discrete Prony* identified model provides significant damping.

The second portion of this dissertation is concerned with control of systems which are modeled through system identification techniques that result in a model with an associated uncertainty set. Control systems are designed so that certain designated signals, such as tracking errors and actuator inputs, do not exceed prespecified levels. Hindering the achievement of this goal are uncertainty about the plant to be controlled and errors in measuring output signals. Uncertainty about the plant is a direct result of the fact that we use mathematical models in representing real physical systems. Furthermore, because sensors can measure signals only to a certain accuracy and because of the natural presence of noise in a system, additional uncertainty through identification occurs in the mathematical modeling process. The issue of uncertainty in the mathematical model leads to the *robust performance problem*, with the goal of achieving specified signal levels in the face of plant uncertainty.

Prior to the 1950s, classical control theory was well established based, in part, on the works of Nyquist [21] and Bode [22]. Following classical methods, control

theory entered the modern control era with emphasis placed on “state-space methods” (a name for all kinds of methodical procedures that has already been used for a long time, e.g., in analytical dynamics, quantum mechanics, theory of stability, in the solution of ordinary differential equations and in other fields). The application of these methods to automatic control was stimulated in the second half of the 1950s mainly by the work of L. S. Pontryagin [23, 24], by the method of dynamic programming as suggested by R. E. Bellman [25] and by the general theory of filtering and control theory elaborated by R. E. Kalman [26]. The recent literature on control systems that is based on state-space methods is very extensive.

Despite the seemingly obvious requirement of bringing plant uncertainty explicitly into control problems, it was only in the early 1980s that ‘modern’ control researchers re-established the link to the classical work of Nyquist, Bode and others by formulating a tractable mathematical notion of uncertainty in an input-output framework and developing rigorous mathematical techniques to cope with it. The basic technique is to model the plant as belonging to a set \mathcal{P} , where such a set can be either *structured* or *unstructured*. The important work of Doyle and Stein [27] established the basic framework for robust control synthesis for systems with unstructured uncertainty.

For an example of a structured set consider the plant model [28]

$$\frac{1}{s^2 + as + 1}$$

This is a standard second-order transfer function with natural frequency 1 rad/sec. and damping ratio $a/2$ – it could represent, for example, a mass-spring damper or an R-L-C circuit. Suppose that the constant a is known only to the extent that it lies in some interval $[a_{min}, a_{max}]$. Then the plant belongs to the structured set

$$\mathcal{P} = \left\{ \frac{1}{s^2 + as + 1} : a_{min} \leq a \leq a_{max} \right\}.$$

For an example of unstructured uncertainty consider the nominal transfer function plant P with the perturbed plant transfer function of the form $\mathcal{P} = \{(1 + \Delta W)P\}$. Here W is a fixed stable transfer function, the weight, and Δ is a variable stable transfer function satisfying $\|\Delta\|_\infty \leq 1$. The uncertainty may be the result of unmodeled dynamics, particularly at high frequency. The infinity-norm on a transfer function is defined as

$$\|G\|_\infty \triangleq \sup_{\omega} |G(j\omega)|$$

and in simple terms says compute the maximum magnitude of the transfer function G over the entire frequency domain (i.e., the maximum gain of the transfer function).

As elaborated in [28], $|W(j\omega)|$ provides the uncertainty profile and at each frequency point the evaluation of \mathcal{P}/P lies in the disk with center 1, radius $|W|$. Typically, $|W(j\omega)|$ is an increasing function of ω such that uncertainty increases with increasing frequency. The main purpose of Δ is to account for phase uncertainty and to act as a scaling factor on the magnitude of the perturbation (i.e., $|\Delta|$ varies between 0 and 1). This type of uncertainty is referred to as multiplicative uncertainty. More detail on other types of frequency domain (*unstructured*) uncertainty can be found in [29, 30] and references therein.

The focus of the robust control research in this dissertation is directed towards those dynamical systems that involve *structured* uncertainty in the form of a bounded ellipsoidal domain on the parameters of the model. In particular, the uncertainty is a direct result of system identification in the presence of noise.

Most identification methods when applied to a set of input/output data provide a model that is usually assumed to be exact for the particular operating point of interest. Quite often, the model is adequate for control design and implementation. In some instances, however, this approach may not be adequate. Thus, we consider the problem where the identified model is given in the form of a nominal set of

parameters including a range of uncertainty associated with the parameters. This type of uncertainty is sometimes referred to as "parametric uncertainty" and indeed falls under the class of *structured uncertainty*.

Recently, the works of [31]-[33] provide system identification methods where the uncertainty on the identified parameters is given in the form of a bounded ellipsoidal region around a nominal set of parameters. The ellipsoid uncertainty region resulting from the method given in [31] is strictly due to additive noise at the output of the system. The method given in [32] and [33] is due to a combination of including a model of unstructured uncertainty in the parameterized model and of additive noise at the output of the system. These methods of identification that result in a nominal set of parameters bounded by an ellipsoidal uncertainty domain are reviewed in Chapter 3.

A brief discussion on set-membership robust control is provided in Chapter 3. Set-membership robust control is simply a control strategy that assumes the system model is given in the form of a nominal set of parameters and an associated bounded uncertainty region. The idea of set-membership control may first have been introduced by Bertsekas and Rhodes in 1971 [34]. While set-membership is a general term, we consider a method of control where the parameters of uncertainty are known to lie within a bounded ellipsoidal domain. Recent results in set-membership control can be found in [35]-[37].

The robust control strategy is approached from a dynamic game theory point of view such that a saddle point solution is desired. For excellent discussion on differential and dynamic game theory see, for example, [38]-[40]. The saddle point is the result of a minimaximization of an energy (cost) function. The game theory method here has two players. Player one is the feedback control signal that attempts to minimize the cost. Player two is the set of uncertain parameters which attempts

to maximize the cost.

It is shown that the optimal control signal necessarily relates to Linear Quadratic Regulation (LQR). The theory of LQR formed a corner stone of the modern control era of the 1960s. The *final cost function* associated with a given plant and the LQR solution provides the means for an iterative approach to the minimaximization solution. The maximization is performed on the *final cost function* and is constrained by the ellipsoidal parameter bound and an appropriate Lyapunov equation from the LQR solution.

An iterative algorithm for both continuous-time and discrete-time systems is developed in Chapter 4. That the fixed-point solution of the algorithm is a saddle point is illustrated by several examples. A sufficient condition for the existence of the maximization portion of the discrete-time algorithm is given.

A closed-loop discrete controlled servo-mechanism example is also provided. The second order system is assumed to be unknown (i.e., a *black box*). Through an identification technique known as the *Optimal Volume Ellipsoid* (OVE) algorithm [31] (discussed in Chapter 3) a model and ellipsoid uncertainty region is found using noisy input/output data. A Kalman filter is used for state estimation. The discrete minimax algorithm is applied to determine the optimal state-feedback gain and the loop is closed. The servo example is stable and shows the worst-case tracking for the noisy, uncertain system. Results are compared to the case where the system is known (i.e., actual plant parameters are used).

A discussion of the results is provided in Chapter 5 and is followed by a section on possible future research in Chapter 6.

CHAPTER 2

DISCRETE PRONY IDENTIFICATION

In this chapter we extend previous results on transfer function identification using Prony signal analysis methods [20]. Recent work resulted in a generalized Prony identification method that incorporates piecewise continuous system input signals; between points of discontinuity, the input is characterized by input eigenvalues and input residues. We refer to the development of [20] as the *continuous Prony* identification method. Here we extend this work to account for sampled-and-held inputs that arise in digital filtering and control. This new method is referred to as *discrete Prony* identification. Using sampled input and output data, initial condition residues are estimated along with transfer function residues and eigenvalues. The two major phases of the *continuous Prony* method are modified to account for the sampled-and-held input; a major contribution is made to the way in which the residues are fit to corresponding eigenvalues in the second phase.

The organization of this chapter is as follows. First, a review of various *parametric* identification techniques is given as a means to establish the category in which Prony identification falls. Following this review of identification techniques the method of *discrete Prony* identification based on Prony signal analysis is presented. The *discrete Prony* algorithm was implemented using MATLAB, and examples are provided. The chapter ends with some concluding remarks.

Review of System Identification Methods

As a means of motivation for this chapter, a review of several methods of identification

is provided. This review is not meant to be exhaustive as this subject area is covered thoroughly in the literature, (e.g., see [1], [41] and [42]).

We can categorize identification methods in a number of ways. In this chapter we consider, among others, the attributes associated with model order selection and whether the method may be used on-line (real-time) or off-line (batch mode). Occasionally, exact knowledge of the system order is known, and identification methods that assume a priori system order should be used. For those situations where exact knowledge of the system order is not known, methods which make no a priori assumption on system order must be used. These methods start over-parameterized and must employ a stage within the identification process where model order selection (reduction) can be accomplished. Methods are available that optimally select the model order of the over-parameterized system. These order selection methods are well suited for on-line identification since they can often be coded. For off-line methods, optimal procedures for model order selection can be used but are not always necessary. Some applications, e.g., those that apply adaptive control require identification methods that can be implemented on-line. The nature of the system and the type of control strategy implemented often will dictate the type of identification to be used; thus, there are always trade-offs between identification schemes.

Identification methods can also be categorized further by considering the effects of noise in the system or the effects of modeled uncertainty. Those models that do not take into account noise are considered deterministic while those that do account for noise are considered stochastic models. Methods of identification that utilize models which include modeled uncertainty are referred to as robust methods of identification.

In the following subsections, we consider two popular models used in the control community and review some of the methods of analysis used to arrive at realizations of the model from the measured input and output data. Following this

review the *continuous Prony* method is introduced and the *discrete Prony* method is developed.

Autoregressive Models (ARX)

Consider the autoregressive model with exogenous input (ARX). The exogenous input is $u : \mathbb{N} \mapsto \mathbb{R}$. Assume that n_a parameters are associated with the AR part of the model, and n_b parameters are associated with the exogenous input. The ARX model is single-input/single-output (SISO) and can be given as

$$\begin{aligned} y(k) &= -\sum_{i=1}^{n_a} a_i y(k-i) + \sum_{j=1}^{n_b} b_j u(k-j) \\ &= \theta^T \phi(k) \end{aligned} \quad (2.1)$$

where the parameter vector to be estimated is

$$\theta^T = [a_1, \dots, a_{n_a}, b_1, \dots, b_{n_b}]$$

and the regression vector containing the past input and output values is given by

$$\phi(k) = [-y(k-1), \dots, -y(k-n_a), u(k-1), \dots, u(k-n_b)]^T.$$

The model order is assumed to be known a priori. Equation (2.1) is considered deterministic since there is no inclusion of noise in the model. The stochastic version can be obtained by introducing an additional noise term, say $\nu(k)$ to the right hand side of (2.1) as seen below.

$$\begin{aligned} y(k) &= -\sum_{i=1}^{n_a} a_i y(k-i) + \sum_{j=1}^{n_b} b_j u(k-j) + \nu(k) \\ &= \theta^T \phi(k) + \nu(k) \end{aligned} \quad (2.2)$$

where θ^T and $\phi(k)$ are defined above.

An expanded version of the ARX model is the autoregressive, moving average model with exogenous input (ARMAX). The moving average part comes from a third

set of parameters operating on the noise terms $\nu(k)$, and is given in (2.3).

$$\begin{aligned} y(k) &= -\sum_{i=1}^{n_a} a_i y(k-i) + \sum_{j=1}^{n_b} b_j u(k-j) + \sum_{l=1}^{n_c} c_l \nu(k-l) + \nu(k) \\ &= \theta^T \phi(k) + \nu(k) \end{aligned} \quad (2.3)$$

where the parameter vector to be estimated is

$$\theta^T = [a_1, \dots, a_{n_a}, b_1, \dots, b_{n_b}, c_1, \dots, c_{n_c}]$$

and the regression vector containing the past input, output and noise values is given by

$$\phi(k) = [-y(k-1), \dots, -y(k-n_a), u(k-1), \dots, u(k-n_b), \nu(k-1), \dots, \nu(k-n_c)]^T.$$

Here the size of the moving average vector, n_c , must be given a priori. Also, past noise terms are seldom known exactly, in which case estimates of them are used in place of actual noise values in the regression vector. It should be noted that the ARMAX model has become a standard tool for both system description and control design.

Least Squares Error Method After the model is established the method of determining the estimate of θ can be formulated. Consider the *least-squares* method. With (2.1) the prediction error becomes

$$\epsilon(k, \theta) = y(k) - \phi^T(k)\theta. \quad (2.4)$$

The *least-squares criterion* for (2.4) is

$$V_N(\theta) = \frac{1}{N} \sum_{k=1}^N \frac{1}{2} [y(k) - \phi^T(k)\theta]^2. \quad (2.5)$$

The *least-squares criterion* is a quadratic function in θ and can be minimized analytically, which gives, provided the indicated inverse exists,

$$\hat{\theta}_N^{LS} = \arg \min_{\theta \in \mathbb{R}} \left[\frac{1}{N} \sum_{k=1}^N \phi(k)\phi^T(k) \right]^{-1} \frac{1}{N} \sum_{k=1}^N \phi(k)y(k) \quad (2.6)$$

the *least-squares estimate* (LSE). From this development, one could introduce different weights on different measurements in the *least-squares criterion* resulting in the *weighted least-squares criterion*.

This method has not appealed to any statistical arguments for the estimation of θ . In fact, the framework of fitting these models to the input/output data makes sense regardless of the stochastic setting. Methods such as *maximum likelihood* are considered statistical parameter estimation techniques. Recursive forms of the ARX/LS and ARMAX/LS methods are available for on-line identification and adaptive control [41]. For a review of these and other methods see [1] and references therein.

State-Space Models

In the state-space form the relationship between the input and output signals is written as a system of first-order differential or difference equations using an auxiliary state vector $\mathbf{x}(t)$. This description of linear dynamical systems became an increasingly dominating approach after Kalman's work in 1960 [43] on prediction and linear quadratic control. This model is especially useful in that insights into physical mechanisms of the system can usually more easily be incorporated into state-space models than into models of the ARX form.

Consider the multi-input multi-output (MIMO) state-space model given by

$$\dot{\mathbf{x}}(t) = A\mathbf{x}(t) + B\mathbf{u}(t), \quad (2.7)$$

where $A \in \mathbb{R}^{n_a \times n_a}$, $B \in \mathbb{R}^{n_a \times m_i}$, the number of inputs is given by m_i and control $\mathbf{u} : \mathbb{R}^+ \mapsto \mathbb{R}^{m_i \times 1}$, and state $\mathbf{x} : \mathbb{R}^+ \mapsto \mathbb{R}^{n_a \times 1}$. The output of the system is given by

$$\mathbf{y}(t) = C\mathbf{x}(t) + D\mathbf{u}(t), \quad (2.8)$$

where $C \in \mathbb{R}^{m_o \times n_a}$ and $D \in \mathbb{R}^{m_o \times m_i}$; the number of outputs is given by m_o .

Consider the single-input single-output (SISO) version of (2.7) and (2.8) with $m_i = m_o = 1$. Let the Laplace transform of $u(t)$ and $y(t)$ be given as $U(s)$ and $Y(s)$, where $s \in \mathbb{C}$. The transfer function of the input/output model from $U(s)$ to $Y(s)$ is given in the Laplace variable s as

$$G(s) = \frac{b_{n_b+1}s^{n_b} + b_{n_b}s^{n_b-1} + b_{n_b-1}s^{n_b-2} + \dots + b_2s + b_1}{s^{n_a} + a_{n_a}s^{n_a-1} + \dots + a_2s + a_1} \quad (2.9)$$

where $n_b \leq n_a$. The poles of (2.9) are defined as the roots of the denominator polynomial which are equivalent to the eigenvalues of A from (2.7). For multi-input multi-output (MIMO) transfer functions and their characteristics, see [44, 45] and references therein.

A discretized version of the continuous time system of equations of (2.7) and (2.8) is given by (2.10) and (2.11) [46]. This discretized version is obtained when the input $u(t)$ is sampled-and-held periodically for a time period T .

$$\mathbf{x}((k+1)T) = F(T)\mathbf{x}(kT) + H(T)\mathbf{u}(kT) \quad (2.10)$$

and

$$\mathbf{y}(kT) = C\mathbf{x}(kT) + D\mathbf{u}(kT). \quad (2.11)$$

Here we have

$$F(T) = e^{AT} \quad (2.12)$$

and

$$H(T) = \left(\int_0^T e^{A\lambda} d\lambda \right) B. \quad (2.13)$$

If matrix A is nonsingular, $H(T)$ given by (2.13) can be simplified to

$$H(T) = A^{-1}(e^{AT} - I)B.$$

Note that the values of C and D of the continuous time state-space model are not affected by the sampled-and-held input signal, $\mathbf{u}(kT)$.

There have been various approaches to system identification using the state-space model. Most of the methods involve extensive use of singular value decomposition (SVD). The derivations of these procedures are relatively lengthy and only a few are described below. It is noted that each of the identification approaches is based on some distinctive method of analysis, as can be seen in the following sections.

Principal Component Analysis Method Consider the approach based on the pulse response matrix of the strictly proper ($D = 0$) discrete system of (2.10) and (2.11). The response $\mathbf{y}(k)$ of the system is given by

$$\mathbf{y}(k) = CF^k\mathbf{x}(0) + \sum_{i=1}^k CF^{i-1}H\mathbf{u}(k-i), k \geq 1. \quad (2.14)$$

The pulse response matrix (also termed Markov parameters) is given by

$$\mathbf{y}_M(k) = CF^{k-1}H, k = 1, 2, \dots \quad (2.15)$$

The system Hankel matrix can be constructed from these Markov parameters as follows

$$\Gamma_{rs}(k-1) = \begin{bmatrix} \mathbf{y}_M(k) & \mathbf{y}_M(k+t_1) & \cdots & \mathbf{y}_M(k+t_{s-1}) \\ \mathbf{y}_M(j_1+k) & \mathbf{y}_M(j_1+k+t_1) & \cdots & \mathbf{y}_M(j_1+k+t_{s-1}) \\ \vdots & \vdots & \ddots & \vdots \\ \mathbf{y}_M(j_{r-1}+k) & \mathbf{y}_M(j_{r-1}+k+t_1) & \cdots & \mathbf{y}_M(j_{r-1}+k+t_{s-1}) \end{bmatrix}$$

where $j_i (i = 1, \dots, r-1)$ and $t_i (i = 1, \dots, s-1)$ are arbitrary integers which can be adjusted to include (or eliminate) specific observations in the Hankel matrix. In [47] a realization (identification) method is developed which provides a full signal model in a single stage, from a single SVD of the system Hankel matrix. Let us suppose for the sake of simplicity that $\Gamma_{rs}(0)$ is a square matrix of order $N = m_o r = m_i s$, where m_o and m_i are defined in (2.7) and (2.8). The SVD then consists of finding an $N \times N$ orthonormal matrix P_N and an $N \times N$ orthonormal matrix Q_N so that

$$\Gamma_{rs}(0) = P_N \Lambda_N Q_N^T$$

with $\Lambda_N = \text{diag}(\lambda_1, \lambda_2, \dots, \lambda_N)$ and $\{\lambda_i\} : \lambda_1 \geq \lambda_2 \geq \dots \geq \lambda_\eta \geq \epsilon \geq \lambda_{\eta+1} \geq \dots \geq \lambda_N \geq 0$. Based on this decomposition, the rank η of $\Gamma_{rs}(0)$ is found as the index of the first nil singular value (for noisy matrices and the relative sizes of the singular values, the nil value is subject to interpretation and is here shown as ϵ).

If the order is chosen as η , the realization becomes

$$F = \Lambda_\eta^{-1/2} P_\eta^T \Gamma_{rs}(1) Q_\eta \Lambda_\eta^{-1/2}$$

$$H = \Lambda_\eta^{1/2} Q_\eta^T E_{m_i}$$

$$C = E_{m_o}^T P_\eta \Lambda_\eta^{1/2}$$

where $E_{m_i}^T = [I_{m_i}, \odot]$ and $E_{m_o}^T = [I_{m_o}, \odot]$. The terms I_{m_i} and I_{m_o} are identity matrices and the term \odot is the null matrix of appropriate dimension. The construction of P_η and Q_η are from P_N and Q_N , respectively; further details can be found in [47].

The method may be considered to be a two-stage algorithm since the model order must be determined prior to calculating the final model. However, once the model order is chosen, all parameters are calculated in one step; thus, the algorithm is, in truth, a single stage algorithm. This approach to system identification, although simple, is not realistic for systems with significant amounts of noise. The model order selection, which is based on the singular values of the Hankel matrix, becomes unreliable under noisy conditions. Also the type of input used for probing is limited to that of a pulse. However, the models to be realized can be SISO, MIMO, or SIMO and are all minimal, which is an advantage over ARX methods.

Canonical Variate Analysis Methods The fundamental concept in the canonical variate analysis (CVA) approach is the *past* and *future* of the process [48], and is based on statistical principles. Associated with each time k is a past vector \mathbf{p}_k consisting of the past outputs and inputs occurring prior to time k as well as a future

vector \mathbf{f}_k consisting of outputs at time k or later,

$$\begin{aligned}\mathbf{p}_k &= [\mathbf{y}^T(k-1), \mathbf{y}^T(k-2), \dots, \mathbf{u}^T(k-1), \mathbf{u}^T(k-2), \dots]^T, \\ \mathbf{f}_k &= [\mathbf{y}^T(k), \mathbf{y}^T(k+1), \dots]^T.\end{aligned}\quad (2.16)$$

The vector processes $\mathbf{y}(k)$ and $\mathbf{u}(k)$ are assumed to be jointly stationary and the covariance matrices among the past \mathbf{p}_k and the future \mathbf{f}_k are denoted as Σ_{ff} , Σ_{pp} , and Σ_{fp} . Now suppose that for a specified state order η , we wish to determine η linear combinations of the past \mathbf{p}_k which allow the optimal prediction of the future \mathbf{f}_k . The set of η linear combinations of the past \mathbf{p}_k is denoted as an $\eta \times 1$ vector \mathbf{m}_k and considered as η -order memory of the past. For any selection of the memory \mathbf{m}_k , the optimal linear prediction $\hat{\mathbf{f}}_k$ is the function [48]

$$\hat{\mathbf{f}}_k(\mathbf{m}_k) = \Sigma_{fm} \Sigma_{mm}^{-1} \mathbf{m}_k \quad (2.17)$$

of the reduced order memory \mathbf{m}_k . The prediction error is measured using the quadratic weighting

$$\mathbb{E}\{\|\mathbf{f}_k - \hat{\mathbf{f}}_k\|_{\Lambda}^2\} = \mathbb{E}\{(\mathbf{f}_k - \hat{\mathbf{f}}_k)^T \Lambda (\mathbf{f}_k - \hat{\mathbf{f}}_k)\} \quad (2.18)$$

where \mathbb{E} is the expectation operation and Λ is an arbitrary positive semidefinite symmetric matrix so that the pseudo-inverse Λ^\dagger is an arbitrary quadratic weighting that is possibly singular. For system identification, the use of the weighting matrix $\Lambda = \Sigma_{ff}$ results in a near maximum likelihood system identification procedure.

In terms of these quantities, the following problem is stated. For a given order η , determine an optimal η -order memory

$$\mathbf{m}_k = J_\eta \mathbf{p}_k \quad (2.19)$$

by choosing the η rows of J_η such that the optimal linear predictor $\hat{\mathbf{f}}_k(\mathbf{m}_k)$ based on \mathbf{m}_k minimizes the prediction error (2.18). The method to arrive at J_η is the subject of

the following discussion. The vector \mathbf{m}_k is intentionally called 'memory' rather than 'state'. A given selection of memory \mathbf{m}_k normally will not correspond to the state of any well defined η -order Markov process. For the system identification problem, this is not a problem since many orders of η will be considered and the one giving the best prediction will be chosen as the optimal order.

Theorem 2.1 (Larimore [48]) Consider the problem of choosing η linear combinations $\mathbf{m}_k = J_\eta \mathbf{p}_k$ of \mathbf{p}_k for predicting \mathbf{f}_k , such that (2.18) is minimized where Σ_{pp} , and Λ are possibly singular positive semidefinite symmetric matrices with ranks m and n respectively. Then the existence and uniqueness of solutions are completely characterized by the (Σ_{pp}, Λ) -generalized singular value decomposition which guarantees the existence of matrices J , L , and generalized singular values $\gamma_1, \dots, \gamma_q$ such that

$$\begin{aligned} J \Sigma_{pp} J^T &= I_m, & L \Lambda L^T &= I_n, \\ J \Sigma_{pf} L^T &= \text{diag}(\gamma_1 \geq \dots \geq \gamma_q > 0, \dots, 0). \end{aligned} \quad (2.20)$$

The solution is given by choosing the rows of J_η if the η -th singular value satisfies $\gamma_\eta > \gamma_{\eta+1}$. If there are r repeated singular values equal to γ_η , then there is an arbitrary selection from among the corresponding singular vectors, i.e. rows of J . Thus, the condition that $\gamma_\eta > \gamma_{\eta+1}$ merely defines a decision point for model order selection. The model order η is to some degree arbitrary, however, the optimal state order can be determined by use of the Akaike information criterion. The minimum value is

$$\min_{\text{rank}(J_\eta \Sigma_{pp} J_\eta^T) = \eta} \mathbb{E}\{\|\mathbf{f}_k - \hat{\mathbf{f}}_k\|_{\Lambda}^2\} = \text{tr} \Lambda^\dagger \Sigma_{ff} - \gamma_1^2 - \dots - \gamma_\eta^2. \quad (2.21)$$

The vectors of variables $\mathbf{c} = J \mathbf{p}_k$ and $\mathbf{d} = L \mathbf{f}_k$ are canonical variables and (2.20) characterizes a *canonical variate analysis*. Now consider the system described by (2.10) and (2.11) where $\mathbf{u}(k)$ and $\mathbf{y}(k)$ are random processes. In [48] models of

noise are included; here we have omitted them for ease of presentation. We wish to model and predict the future of $\mathbf{y}(k)$ by an η -state $\mathbf{x}(k)$. The particular multivariate regression equations are expressed in terms of covariances, denoted by Σ , among various vectors as

$$\begin{bmatrix} F & H \\ C & D \end{bmatrix} = \Sigma \left[\begin{pmatrix} \mathbf{m}(k+1) \\ \mathbf{y}(k) \end{pmatrix}, \begin{pmatrix} \mathbf{m}(k) \\ \mathbf{u}(k) \end{pmatrix} \right] \Sigma^{-1} \left[\begin{pmatrix} \mathbf{m}(k) \\ \mathbf{u}(k) \end{pmatrix}, \begin{pmatrix} \mathbf{m}(k) \\ \mathbf{u}(k) \end{pmatrix} \right]. \quad (2.22)$$

Explicit computation is obtained by the substitution of $\mathbf{m}_k = J_\eta \mathbf{p}_k$.

To decide on the model state order or model structure, recent developments based upon entropy or information measures are used. Such methods were originally developed by Akaike [49] and involve the use of the Akaike Information Criterion (AIC) for deciding the appropriate order of a statistical model. In simplest terms the AIC is a procedure that minimizes negative entropy. The AIC for each order η is defined by

$$AIC(\eta) = -2 \log p(Y^N, U^N; \hat{\theta}_\eta) + 2M_\eta \quad (2.23)$$

where p is the likelihood function based on the observations (Y^N, U^N) at N time points, and where $\hat{\theta}_\eta$ is the maximum likelihood parameter estimate using an η -order model with M_η parameters. For more information on likelihood functions see [1, pages 181-190]. The model order η is chosen corresponding to the minimum value of the $AIC(\eta)$. The number of parameters in (2.10) and (2.11) is

$$M_\eta = (2\eta + m_i)m_o + m_i m_o + m_o(m_o + 1)/2$$

where m_i and m_o are the number of input and output variables, respectively. This result is developed by considering the size of the equivalent class of state space models having the same input/output and noise characteristics [50]. Thus the number of functionally independent parameters in a state-space model is far less than the number of elements in the various state-space matrices. Effectively, the AIC imposes a statistical penalty on the order (parameter size) of the model.

State Variable Analysis Methods An approach that is in some ways similar to CVA, referred to as State Variable Analysis (SVA), attempts to estimate the state of the system, and from the state, produce a realization of the state-space model. A particular formulation of an SVA algorithm is given in [51] and is briefly discussed as follows. First, a time-series state-vector basis for the dynamical system is realized as the intersection of the row spaces of two block Hankel matrices constructed with measured input/output (I/O) data. This step is done by repeated use of SVD. The second step solves a set of linear equations for F , H and C . The set of linear equations for step two is constructed from the basis vector estimated in step one.

The algorithm assumes that the data are consistent with the discrete-time state-space model of (2.10) and (2.11). The algorithm utilizes a Hankel matrix Υ ,

$$\Upsilon = \begin{bmatrix} \Upsilon_1 \\ \Upsilon_2 \end{bmatrix} \quad (2.24)$$

where

$$\Upsilon_1 = \begin{bmatrix} \mathbf{u}(k) & \mathbf{u}(k+1) & \cdots & \mathbf{u}(k+j-1) \\ \mathbf{y}(k) & \mathbf{y}(k+1) & \cdots & \mathbf{y}(k+j-1) \\ \mathbf{u}(k+1) & \mathbf{u}(k+2) & \cdots & \mathbf{u}(k+j) \\ \mathbf{y}(k+1) & \mathbf{y}(k+2) & \cdots & \mathbf{y}(k+j) \\ \vdots & \vdots & \ddots & \vdots \\ \mathbf{u}(k+i-1) & \mathbf{u}(k+i) & \cdots & \mathbf{u}(k+j+i-2) \\ \mathbf{y}(k+i-1) & \mathbf{y}(k+i) & \cdots & \mathbf{y}(k+j+i-2) \end{bmatrix}$$

and

$$\Upsilon_2 = \begin{bmatrix} \mathbf{u}(k+i) & \mathbf{u}(k+i+1) & \cdots & \mathbf{u}(k+j+i-1) \\ \mathbf{y}(k+i) & \mathbf{y}(k+i+1) & \cdots & \mathbf{y}(k+j+i-1) \\ \mathbf{u}(k+i+1) & \mathbf{u}(k+i+2) & \cdots & \mathbf{u}(k+j+i) \\ \mathbf{y}(k+i+1) & \mathbf{y}(k+i+2) & \cdots & \mathbf{y}(k+j+i) \\ \vdots & \vdots & \ddots & \vdots \\ \mathbf{u}(k+2i-1) & \mathbf{u}(k+2i) & \cdots & \mathbf{u}(k+j+2i-2) \\ \mathbf{y}(k+2i-1) & \mathbf{y}(k+2i) & \cdots & \mathbf{y}(k+j+2i-2) \end{bmatrix}$$

Application of singular value decomposition is used to estimate a basis, X , from which the time-series state vector can be obtained. It is shown in [51] that

$$\text{span}_{\text{row}}(X) = \text{span}_{\text{row}}(\Upsilon_1) \cap (\Upsilon_2),$$

where the basis, X , is given as

$$X = [\mathbf{x}_{k+i} \ \mathbf{x}_{k+i+1} \ \dots \ \mathbf{x}_{k+i+j-2}].$$

Note, we have replaced $\mathbf{x}(k)$ with subscript notation \mathbf{x}_k . As stated in [51], i and j should be chosen sufficiently large (insuring sufficient information about the system), and $j \gg i$ so that computational load and noise sensitivity are reduced. With the state-vector basis determined the order of the system must be decided before the state-space matrices of (2.10) and (2.11) can be estimated. If the system is completely noise free the singular values of the SVD will reveal the exact order of the system. If noise is present one must observe the relative magnitudes of the singular values and determine an appropriate order for the model. This problem of the effect of noise on the singular values of the system Hankel matrix has been addressed in [52]. In [52] it is shown that small perturbations in the input and output matrices H and C can reveal those modes that are associated with the actual system and those modes associated with noise. Also, a selection procedure similar to the AIC may be employed for model order reduction.

With the order and resulting basis X established, the following set of linear equations may be solved in a least-squares sense for F , H , C and D .

$$\begin{bmatrix} X_{k+i+1}, \dots, X_{k+j+i-1} \\ \mathbf{y}_{k+i}, \dots, \mathbf{y}_{k+j+i-2} \end{bmatrix} = \begin{bmatrix} F & H \\ C & D \end{bmatrix} \begin{bmatrix} X_{k+i}, \dots, X_{k+j+i-2} \\ \mathbf{u}_{k+i}, \dots, \mathbf{u}_{k+j+i-2} \end{bmatrix}. \quad (2.25)$$

This method can be adapted for on-line identification.

This review has described some of the modern techniques of identification being used and it revealed issues that one must be concerned with when choosing a method. Each of the methods was presented in its simplest form. Each method has been extended to account for various types of noise, see, e.g., [53, 54]. Following is the development of the *discrete Prony* method. At the end of this chapter *discrete Prony* will be compared to the SVA method just described.

Prony Signal Identification for Discrete Control Systems

Introduction: Discrete Prony

The Prony method for system identification is based on a signal analysis method for approximating a signal with a weighted sum of exponentials. A complete survey of the development and uses of Prony methods in system identification is given in [20]. Since the original work of Prony [2], much has been accomplished in the way of system identification based on this analysis technique.

Most recently [20] has provided a general Prony approach for system identification where the probing input is piecewise continuous; between points of discontinuity, the input is characterized by input eigenvalues and input residues. The procedure is given in essentially two steps: a) modal (eigenvalue) identification and b) residue fitting. Within each of these steps there are additional steps that can be taken to aid in the final transfer function model optimal selection. The method results in estimates of initial condition residues, transfer-function residues, and system eigenvalues. The development in [20] is set in the continuous time domain and leads to a relatively complicated procedure in step b.

Unlike the method in [20] the development here is for those systems that are implemented using sampled-and-held inputs. This development leads to a straightforward procedure for step b.

System Characterization

System Model The system model shown in Figure 1 is a SISO system. Through partial fraction expansion the system model from (2.9) has the Laplace transform function represented in standard parallel form:

$$\hat{G}(s) = R_0 + \sum_{j=1}^{\eta} \frac{R_j}{s - \xi_j}. \quad (2.26)$$

In Figure 1 the initial condition terms are included explicitly in the summation preceding the output $\hat{y}(t)$, so that the input $u(t)$ can be taken as 0 for $t < 0$. The input $u(t)$ is sampled-and-held prior to its application to both the model and the system. The constant sample period is T . Although a zero-order-hold (ZOH) circuit is indicated in Figure 1, the approach that follows can be modified to account for other hold circuits. The ξ_j 's are the eigenvalues of the system model, R_0 is a feed-through gain, R_1 through R_η are the model residues, and E_1 through E_η are initial condition residues. The ξ_j 's are assumed to be distinct and can occur in complex conjugate pairs. Residues corresponding to complex conjugate eigenvalues also occur in complex conjugate pairs. The objective of the identification procedure is to find values of ξ_j 's, R_j 's, E_j 's and η so that the model's output $\hat{y}(t)$ is close as possible, in some appropriate sense, to the actual system output $y(t)$.

If there is a dc offset in the output, then some ξ_j will equal zero with the associated $E_j \neq 0$; and if there is no eigenvalue with value zero in $G(s)$, then the associated $R_j \cong 0$.

General System Input For the identification method that is developed in this thesis, the input $u(t)$ for $t \geq 0$ is assumed to be of the general form:

$$u(t) = \sum_{k=1}^q \sum_{l=1}^{m_k} c_{k,l} (e^{\mu_{k,l}(t-\tau_{k-1})}) [u_s(t - \tau_{k-1}) - u_s(t - \tau_k)], \quad (2.27)$$

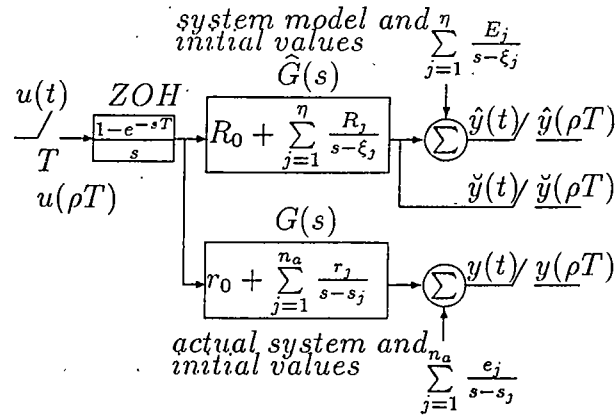


Figure 1. System and actual model in parallel form.

which is discontinuous at a finite number $q + 1$ points in time. Here the step function is represented by $u_s(\cdot)$. The k^{th} input time interval is characterized by $t \in [\tau_{k-1}, \tau_k)$ where $\tau_0 = 0$ without loss of generality. A total of $q + 1$ time intervals exist for $t \geq 0$, where the $(q + 1)^{\text{th}}$ time interval corresponds to $t \geq \tau_q$ in which $u(t) = 0$.

For each input interval, $(\tau_k - \tau_{k-1})/T$ is assumed to be an integer value. Let the integer M_k be defined by

$$M_k \triangleq \frac{\tau_k}{T}, \quad k = 0, 1, \dots, q.$$

The input time intervals can be characterized in terms of the M_k 's: letting $t = \rho T$, $\rho = 0, 1, \dots$, the input time interval is characterized by integer time $\rho \in [M_{k-1}, M_k)$ for $k = 1, 2, \dots, q$. During the k^{th} time interval, the input signal is characterized by the set of input eigenvalues $\{\mu_{k,l}\}_1^{m_k}$ with corresponding amplitude set $\{c_{k,l}\}_1^{m_k}$. The input eigenvalues can be selected to excite specific frequency ranges of interest. All values of the input signal parameters are assumed known.

Output Response Using $u(t)$ of (2.27) as the input in Figure 1, the model output $\hat{y}(t)$ is given by

$$\hat{y}(t) = \sum_{j=1}^{\eta} E_j e^{\xi_j t} + \check{y}(t), \quad (2.28)$$

where $\check{y}(t)$ is shown in Figure 1.

In order to employ the method of Prony in modal identification a thorough understanding of the sampled output signal in terms of the input and system modes is necessary. The analysis can be quite tedious because the system is being driven by a zero-order hold circuit and the input signal is piece-wise continuous. Therefore, for purposes of explanation, consider a first-order model

$$\hat{G}(s) = \frac{R}{s - \xi},$$

with initial conditions IC,

$$IC(s) = \frac{E}{s - \xi}.$$

Allow the input to be given by

$$u(t) = e^{\mu(t-\tau_{k-1})} [u_s(t - \tau_{k-1}) - u_s(t - \tau_k)]. \quad (2.29)$$

The following derivations make use of various properties and theorems of the z-transform and may be found in [46, pages 51-57, 86 and 152]. Let the z-transform operator be represented by $\mathcal{Z}\{\cdot\}$; then the z-transform of the input of (2.29) is

$$U(z) = \mathcal{Z}\{u(t)\} = z^{-M_{k-1}} [1 - z^{-\Delta_M} \gamma^{\Delta_M}] \frac{z}{z - \gamma}, \quad (2.30)$$

where

$$\Delta_M \triangleq M_k - M_{k-1} \text{ and } \gamma \triangleq e^{\mu T}.$$

The z-transform of IC(s) is

$$IC(z) = \mathcal{Z}\left\{\frac{E}{s - \xi}\right\} = E \frac{z}{z - \lambda}, \quad (2.31)$$

where

$$\lambda \triangleq e^{\xi T}.$$

Next, consider Figure 1 and (2.30) and (2.31); then the z-transform of $\hat{y}(t)$ is given by

$$\begin{aligned} \hat{Y}(z) &= IC(z) + U(z)(1 - z^{-1})\mathcal{Z}\left\{\frac{R}{s(s - \xi)}\right\} \\ &= E\frac{z}{z - \lambda} + z^{-M_{k-1}}[1 - z^{-\Delta_M}\gamma^{\Delta_M}]\frac{\frac{R}{\xi}(\lambda - 1)z}{(z - \lambda)(z - \gamma)}. \end{aligned} \quad (2.32)$$

There are three cases to consider when analyzing the output signal.

Case 1) $\rho: \rho T < M_{k-1}T$

It can be seen from (2.32) that the only part of $\hat{Y}(z)$ that has nonzero inverse when $\rho < M_{k-1}$ is

$$E\frac{z}{z - \lambda},$$

and thus

$$\hat{y}(\rho T) = E\lambda^\rho, \quad \rho < M_{k-1}.$$

Case 2) $\rho: M_{k-1}T \leq \rho T < M_k T$

In this case, those parts of $\hat{Y}(z)$ having nonzero inverse terms over the time interval are

$$E\frac{z}{z - \lambda} + z^{-M_{k-1}}\frac{\frac{R}{\xi}(\lambda - 1)z}{(z - \lambda)(z - \gamma)}$$

and thus

$$\hat{y}(\rho T) = E\lambda^\rho + \frac{R(\lambda - 1)}{\xi(\lambda - \gamma)}[\lambda^{\rho - M_{k-1}} - \gamma^{\rho - M_{k-1}}], \quad M_{k-1} \leq \rho < M_k. \quad (2.33)$$

Case 3) $\rho: \rho T \geq M_k T$

It can be seen from (2.32) and (2.33) that $\hat{y}(\rho T)$ takes on the following form

$$\hat{y}(\rho T) = E\lambda^\rho + \frac{R(\lambda - 1)}{\xi(\lambda - \gamma)}[\lambda^{\rho - M_{k-1}} - \gamma^{\Delta_M}\lambda^{\rho - M_k}], \quad \rho \geq M_k.$$

Hence, it can be seen that while the input is off the output signal contains only those modes associated with the system, whereas, while the input is on, as in case 2, the output signal is comprised of input and system modes. Further note that in case 3 the modal content of the output signal is comprised of linear combinations of the system mode, λ , where the constant multipliers of this system mode are a function of the past input mode, γ .

In general it can be said that during a given interval k the modal content of the output signal consists of linear combinations of both the input and system modes, and while the input is off, the modal content of the output signal consists of linear combinations of the system modes.

Thus, for any interval defined by $[\tau_{k-1}, \tau_k)$ such that the probing input is on, (i.e. for $k = 1, 2, \dots, q$), the part of $\hat{Y}(z)$ that has a nonzero inverse can be characterized by

$$[\hat{Y}(z)]_k \triangleq \left[\frac{n_{\hat{y}}(z^{-1})}{d_{\hat{y}}(z^{-1})} \right]_k = \frac{[n_{\hat{y}}(z^{-1})]_k}{d_{\hat{G}}(z^{-1}) [d_u(z^{-1})]_k}, \quad (2.34)$$

where $d_{\hat{G}}(z^{-1})$ is the characteristic polynomial of the model, $[d_u(z^{-1})]_k$ is the characteristic polynomial for the input over the k^{th} interval and $[n_{\hat{y}}(z^{-1})]_k$ is an appropriate numerator polynomial. Otherwise, for $k = q + 1$ or while the input is off

$$[\hat{Y}(z)]_k = \frac{[n_{\hat{y}}(z^{-1})]_k}{d_{\hat{G}}(z^{-1})}. \quad (2.35)$$

From (2.34) it can be seen that the modal content of the sampled output signal consists of a combination of input and system modes, whereas, from (2.35) the modal content of the sampled output signal consists only of those contributed by the system.

Prony Based Analysis

Basic Properties The objective of the first step of Prony analysis is to find the eigenvalues of the sampled output signal $y(t)$. We assume that the signal $y(t)$ is

sampled at a sample period T smaller than the Nyquist period. During the k^{th} time interval the sampled signal $\hat{y}(\rho T)$ can be rewritten in discrete-time form as

$$\hat{y}_\rho = \sum_{i=1}^{\nu_k} \beta_{k,i} z_i^{\rho - M_{k-1}}, \quad \rho = M_{k-1}, \dots, M_k - 1,$$

where ρ is integer time, $\hat{y}_\rho \equiv \hat{y}(\rho T)$, $\beta_{k,i} \in \mathbb{C}$ for $i = 1, 2, \dots, \nu_k$, $\nu_k \triangleq \eta + m_k$, and each z_i is a discrete-time eigenvalue of the system or of the input. It is well known that \hat{y}_ρ satisfies its own characteristic equation, [2, 9]; thus from (2.34) and (2.35), it follows that

$$[d_{\hat{y}}(z^{-1})]_k \hat{y}_\rho \cong 0, \quad \rho = M_{k-1} + \nu_k, \dots, M_k - 1, \quad (2.36)$$

where the characteristic polynomial of (2.34) and (2.36) is defined as

$$[d_{\hat{y}}(z^{-1})]_k \triangleq 1 - (\phi_{k,1} z^{-1} + \phi_{k,2} z^{-2} + \dots + \phi_{k,\nu_k} z^{-\nu_k}). \quad (2.37)$$

Thus, for $\rho \in [M_{k-1} + \eta + m_k, M_k - 1]$, where the definition for ν_k has been substituted, we have from (2.36) and (2.37)

$$\hat{y}_\rho \cong \phi_{k,1} \hat{y}_{\rho-1} + \phi_{k,2} \hat{y}_{\rho-2} + \dots + \phi_{k,\nu_k} \hat{y}_{\rho-\nu_k}. \quad (2.38)$$

Allowing ρ to range over the defined interval and substituting y_ρ for \hat{y}_ρ provides a system of over-determined linear equations (i.e., more parameters than necessary to describe the 'true' system) that can be solved in a least-squares sense for the coefficients $\phi_{k,i}$. Factoring (2.37) then results in estimates for the eigenvalues of the signal. By removing the eigenvalues $\{\mu_{k,l}\}_1^{m_k}$ associated with the input signal, the desired estimates for the eigenvalues $\{\xi_j\}_1^\eta$ of the system are obtained along with residual eigenvalues due to the over-determination.

Modal Identification Three different approaches to obtaining the set $\{\xi_j\}_1^\eta$ are described in detail in [20] and are referred to as i) Separate least-squares solutions; ii) Combined least-squares solution for system eigenvalues; and iii) Combined

least-squares solution for all eigenvalues. Equations (2.36) - (2.38) are the basis for method i.

The second approach provides a good degree of insight to the first stage of Prony analysis and will be discussed below. Method ii requires the construction of auxiliary equations with knowledge of the input signal and solves directly for the system eigenvalues, ξ_j 's. Let the characteristic polynomial of the system be given by

$$d_{\hat{G}}(z^{-1}) \triangleq 1 - (\psi_1 z^{-1} + \psi_2 z^{-2} + \dots + \psi_\eta z^{-\eta}) \quad (2.39)$$

and in factored form

$$d_{\hat{G}}(z^{-1}) \equiv \prod_{j=1}^{\eta} (1 - e^{\xi_j T} z^{-1}). \quad (2.40)$$

The characteristic polynomial of the input for the k^{th} interval is given by

$$[d_u(z^{-1})]_k \triangleq 1 + \alpha_{k,1} z^{-1} + \alpha_{k,2} z^{-2} + \dots + \alpha_{k,m_k} z^{-m_k}$$

and in factored form

$$[d_u(z^{-1})]_k \equiv \prod_{l=1}^{m_k} (1 - e^{\mu_{k,l} T} z^{-1}). \quad (2.41)$$

Over the k^{th} time interval, from (2.34) we have

$$d_{\hat{G}}(z^{-1}) ([d_u(z^{-1})]_k y_\rho) \cong 0$$

or

$$d_{\hat{G}}(z^{-1}) p_k(\rho) \cong 0, \quad (2.42)$$

where $p_k(\rho)$ is generated based on the known $[d_u(z^{-1})]_k$ of (2.41). The form of $p_k(\rho)$ is given by

$$p_k(\rho) = y_\rho + \alpha_{k,1} y_{\rho-1} + \alpha_{k,2} y_{\rho-2} + \dots + \alpha_{k,m_k} y_{\rho-m_k}, \quad (2.43)$$

where $\rho \in [M_{k-1} + m_k, M_k - 1]$. Using (2.39), (2.42) and (2.43), and appropriately narrowing the range on ρ , we have

$$p_k(\rho) \cong \psi_1 p_k(\rho - 1) + \psi_2 p_k(\rho - 2) + \dots + \psi_\eta p_k(\rho - \eta), \quad (2.44)$$

where $\rho \in [M_{k-1} + m_k + \eta, M_k - 1]$.

For some input interval, say $k = r$; if $M_r - 1$ is less than $M_{r-1} + m_r + \eta$, then the r^{th} interval of data cannot be used in the construction of the above set of equations. Also, for interval $k = q + 1$ or any interval where the input $u(t) = 0$, it follows from (2.35) and (2.39) that

$$y_\rho \cong \psi_1 y_{\rho-1} + \psi_2 y_{\rho-2} + \cdots + \psi_\eta y_{\rho-\eta}, \quad (2.45)$$

where

$$\rho : \begin{cases} \rho \in [M_{k-1} + \eta, M_k - 1] & \text{if } u(t) = 0, \\ \rho \geq M_{k-1} + \eta & \text{if } k = q + 1. \end{cases}$$

The unknowns in (2.44) and (2.45) are the ψ_i 's. For each time interval of sufficient width, and where $u(t) \neq 0$, a set of linear equations in the following form result:

$$\mathbf{v}_k \cong \Phi_k \psi, \quad (2.46)$$

where $\psi \in \mathbb{R}^\eta$ consists of ψ_i 's, the Toeplitz matrix $\Phi_k \in \mathbb{R}^{(M_k - M_{k-1} - m_k - \eta, \eta)}$ consists of appropriate ordering of $p_k(\rho - 1), \dots, p_k(\rho - \eta)$, and $\mathbf{v}_k \in \mathbb{R}^{(M_k - M_{k-1} - m_k - \eta)}$ consists of appropriate ordering of $p_k(\rho)$. For intervals where $u(t) = 0$ or $k = q + 1$, we have the same ψ , however, the Toeplitz matrix $\Phi_k \in \mathbb{R}^{(M_k - M_{k-1} - \eta, \eta)}$ and $\mathbf{v}_k \in \mathbb{R}^{(M_k - M_{k-1} - \eta)}$ each consist of appropriate ordering of y_ρ . As suggested in [20], it may be necessary for numerical reasons to row scale each interval set of equations such that the matrices have same order of magnitude. In any case, with all input intervals of sufficient length used in (2.46) the concatenation results in an over-determined set of equations:

$$\mathbf{v} \cong \Phi \psi.$$

To arrive at a set of parameters ψ_j 's, the following least-squares problem can be solved

$$\psi = \arg \min_{\psi} \|\mathbf{v} - \Phi \psi\|_2.$$

Once ψ is determined, a high precision root-finding algorithm or eigenvalue solving algorithm can be used to factor $d_{\hat{G}}(z^{-1})$ of (2.39) to obtain $z_j \triangleq e^{\xi_j T}$, (the roots of (2.40)). It is then a simple matter to solve for the set, $\{\xi_j\}_1^\eta$.

Residue Fitting With the first phase of Prony identification resulting in the set of ξ_j 's it remains to estimate the R_j 's and E_j 's. Equation (2.26) can be rewritten as

$$\hat{G}(s) = R_0 + \sum_{j=1}^{\eta} \hat{G}_j(s), \quad (2.47)$$

where $\hat{G}_j(s) \triangleq \frac{R_j}{s - \xi_j}$.

Each subsystem $\hat{G}_j(s)$ can be written in state-space parameters as

$$\hat{G}_j(s) = C_j(sI - A_j)^{-1}B_j + D_j,$$

where $A_j = \xi_j$, $D_j = 0$ and we are free to choose $B_j = 1$ and $C_j = R_j$ for all j . Next, recall that the system has been probed by an input signal which has been sampled-and-held, thus the discretization of $\hat{G}_j(s)$ (see (2.10) and (2.11)) is given by

$$\mathbf{x}_j((\rho + 1)T) = F_j(T)\mathbf{x}_j(\rho T) + H_j(T)u(\rho T) \quad (2.48)$$

and

$$\check{y}_j(\rho T) = R_j\mathbf{x}_j(\rho T). \quad (2.49)$$

Here we have

$$F_j(T) = e^{\xi_j T} \quad (2.50)$$

and

$$H_j(T) = \int_0^T e^{\xi_j t} dt. \quad (2.51)$$

If $\xi_j \neq 0$

$$H_j(T) = \frac{e^{\xi_j T} - 1}{\xi_j}$$

otherwise

$$H_j(T) = T.$$

From (2.28) and (2.49) the estimate of the output can be written as

$$\hat{y}(\rho T) = \sum_{j=1}^{\eta} \check{y}_j(\rho T) + R_0 u(\rho T) + \sum_{j=1}^{\eta} E_j e^{\xi_j \rho T},$$

where $\rho = 0, 1, 2, \dots, N$. The problem statement can be stated in the following form:

$$[R, E] = \arg \min_{[R, E]} \|y - \hat{y}\|_2. \quad (2.52)$$

Using (2.48) - (2.51), let ε be defined by

$$\varepsilon \triangleq y - [\Theta_1 \ \Theta_2] \begin{bmatrix} R \\ E \end{bmatrix}, \quad (2.53)$$

where

$$R \equiv [R_0 \ R_1 \ \dots \ R_\eta]^T,$$

$$E \equiv [E_1 \ E_2 \ \dots \ E_\eta]^T,$$

$$y \equiv [y(0) \ y(T) \ \dots \ y(NT)]^T,$$

$$\Theta_1 \equiv \begin{bmatrix} u(0) & x_1(0) & \dots & x_\eta(0) \\ u(T) & x_1(T) & \dots & x_\eta(T) \\ \vdots & \vdots & \ddots & \vdots \\ u(NT) & x_1(NT) & \dots & x_\eta(NT) \end{bmatrix}$$

and

$$\Theta_2 \equiv \begin{bmatrix} 1 & 1 & \dots & 1 \\ z_1 & z_2 & \dots & z_\eta \\ z_1^2 & z_2^2 & \dots & z_\eta^2 \\ \vdots & \vdots & \ddots & \vdots \\ z_1^N & z_1^N & \dots & z_\eta^N \end{bmatrix}$$

Thus, (2.52) can be re-stated as

$$[R, E] = \arg \min_{[R, E] \in \mathbb{R}} \|\varepsilon\|_2. \quad (2.54)$$

Determination of Model Order η There are various methods of determining the optimal order selection η . Using the parsimony principle [42], the best model of a system is defined as the one that accurately represents a transfer function with a minimal number of parameters. Using Prony, the first phase estimates a large number of modes and then performs various reduction procedures to arrive at an optimal order selection. The first phase invariably places many discrete-poles in the 2nd and 3rd quadrants of the complex z-plane. These poles relate to modes that are near the Nyquist rate and often may be discarded.

Once a set of modes is selected the residues are fit to these modes as described above. An ordering algorithm is applied to this set of mode/residue pairs. An ordering scheme proposed in [55] provides a practical approach. The method sequentially compares subsets of mode/residue pairs by a given error criterion. The mode/residue pairs that provide the least amount of error are placed at the top of the order and new subsets are formed. An outline of the ordering algorithm used is as follows.

I. Define:

- (a) Each real eigenvalue and its associated residue constitute a mode/residue pair. For complex conjugate eigenvalues, we use the same terminology, mode/residue pair, to denote a complex conjugate pair of eigenvalues and their associated complex-conjugate residues. Let M denote the number of mode/residue pairs.
- (b) The ordering-criterion is based on the minimization of the relative error between the actual output and the estimated output over combinations of mode/residue pairs.
- (c) The error-criterion is the relative error between the actual output and the estimated output.

II. Let $k=1$.

- (a) Evaluate the relative error for each of the mode/residue pairs according to the error-criterion.
- (b) Order each of these mode/residue pairs according to the ordering-criterion.
- (c) Place the mode/residue pair associated with the minimum in a separate list defined as the sorted-set. The remaining $M-1$ residue/pairs are placed in a second list defined as the remaining-set.
- (d) $k = k + 1$.

III. While $k < M$

- (a) Construct $M - k$ combinations with each combination consisting of the sorted-set and one mode/residue pair of the remaining-set.
- (b) Evaluate the relative error for each of the $M - k$ combinations according to the error-criterion.
- (c) Order each of these combinations according to the ordering-criterion.
- (d) Place the mode/residue pair associated with the combination that gives the minimum in the sorted-set. The remaining $M - k$ mode/residue pairs constitute the remaining-set.
- (e) $k = k + 1$.

IV. end

The final choice of model order is established when the change in error from one pair to the next is insignificant. For more detail on this approach see [55].

A method based upon objective entropy or information measures can be used to optimally decide on the model state order [54]. The Akaike information criterion (AIC) [49] minimizes the Kullback discrimination information [56]. The resulting error criterion includes a penalty on the order number which lends itself well to automated optimal order selection. This approach is well suited for various identification approaches. In regard to Prony identification and model order selection, the reader is referred to [57].

An automated procedure to determine model order is not employed in the examples that follow. Instead, plots of the error in dB vs number of modes are constructed and used to note the point of diminishing return (no significant improvement on error) as the model order increases.

Examples

For our examples the linear system "benchmark" of [58] is used and is shown in Figure 2. Three examples are provided. The first example is noise free. The second example is the same as the first except for the addition of white noise to the measured output.

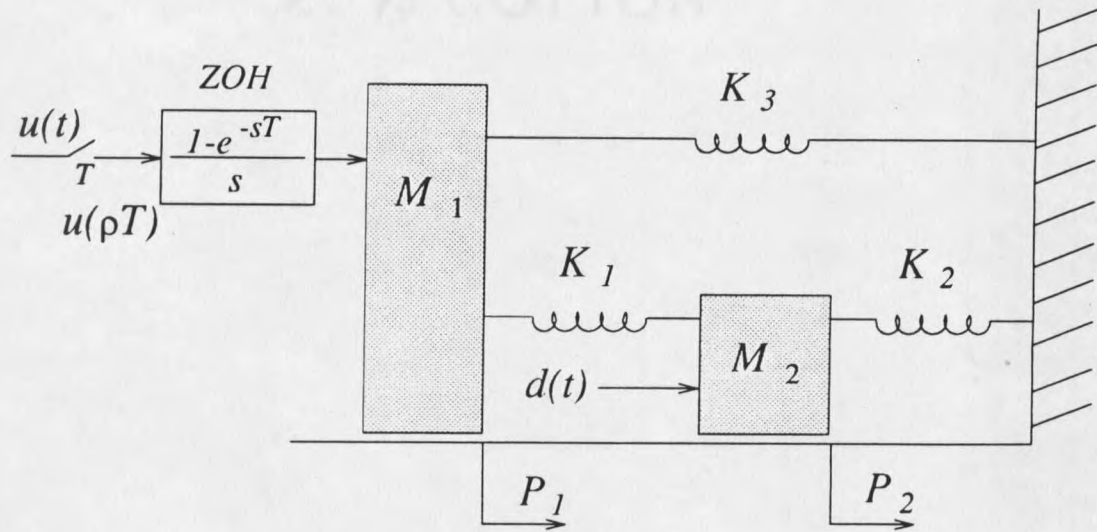


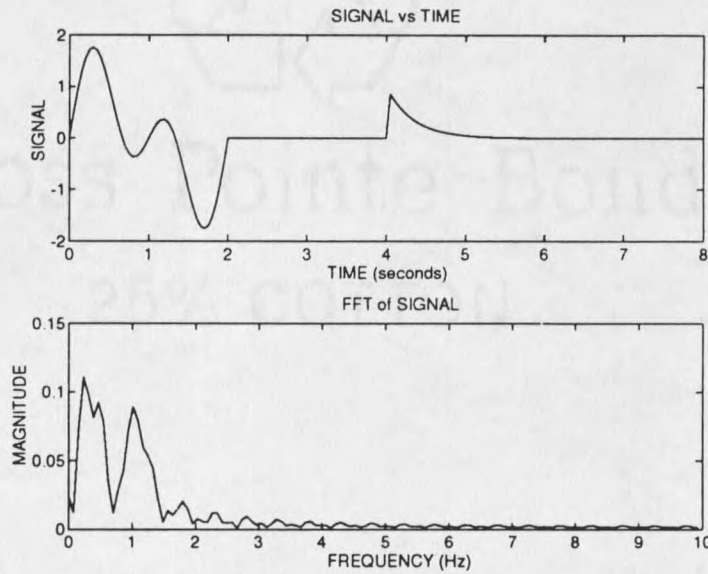
Figure 2. The linear mass/spring diagram for Examples 1-3.

In the third example, both the *discrete Prony* algorithm and an SVA method are applied and compared under conditions of additive white process noise. The system of Figure 2 conforms to that of Figure 1 for specified values of system parameters and initial conditions, as are listed in Table 1. The input drive signal for Examples 1 and 2, shown in Figure 3, is described in Table 2. The input drive signal was chosen in somewhat of an arbitrary fashion to show the variety of input drive signals the *discrete Prony* method can handle. The system is known to have modal content below the 3 Hz range, and the frequency content of the drive signal, as shown in Figure 3, is adequate for Examples 1 and 2. The system output $y(t)$ in all examples is $P_1(t)$ of Figure 2. In Examples 1 and 2, $d(t) = 0$ in Figure 2.

Example 1: No Noise Case For the first example white noise was not added to the measured output. An initial model order η of 30 was chosen prior to applying the Prony identification technique. After the first phase of Prony was complete, 14 of the 30 modes found were in the 1st or 4th quadrant of the z -plane.

j	s_j	r_j	e_j
1	-31.400	-0.9863	0.3000
2	-0.2500	0.0031	0.1000
3,4	-0.0500 $\pm 5.7276i$	0.3034 $\mp 0.0392i$	0.2000 $\mp 0.1000i$
5,6	-0.0500 $\pm 3.4913i$	0.1882 $\mp 0.0047i$	0.0500 $\mp 0.2000i$

Table 1. Actual system model data for Examples 1-3.

Figure 3. Probing input $u(t)$ and its Fourier transform equivalent for Examples 1-2.

$\tau_1 = 2$ seconds $m_1 = 4$ modes			$\tau_2 = 4$ seconds $m_2 = 0$ modes			$\tau_3 = 6$ seconds $m_3 = 1$ mode		
l	$\mu_{1,l}$	$c_{1,l}$	l	$\mu_{2,l}$	$c_{2,l}$	l	$\mu_{3,l}$	$c_{3,l}$
1	$3.1416i$	$-0.5000i$				1	-3.0000	+1.0000
2	$-3.1416i$	$+0.5000i$						
3	$6.2832i$	$-0.5000i$						
4	$-6.2832i$	$+0.5000i$						

Table 2. Input drive data for Examples 1-2.

j	ξ_j	R_j	E_j	error(dB)
1,2	$-5.0000e - 02$ $\mp 5.7276e + 00i$	$3.0338e - 01$ $\pm 3.9152e - 02i$	$2.0000e - 01$ $\pm 1.0000e - 01i$	-3.7748e+00
3,4	$-5.0000e - 02$ $\mp 3.4914e + 00i$	$1.8817e - 01$ $\pm 4.7146e - 03i$	$5.0000e - 02$ $\pm 2.0000e - 01i$	-2.0229e+01
5	$-2.5000e - 01$	$3.1427e - 03$	$1.0000e - 01$	-2.6472e+01
6	$-3.1400e + 01$	$-9.8626e - 01$	$3.0000e - 01$	-1.9910e+02
7,8	$-8.6376e - 01$ $\mp 1.3699e + 01i$	$-4.5645e - 11$ $\pm 2.0300e - 10i$	$-1.1734e - 11$ $\pm 1.0299e - 11$	-2.0103e+02
9,10	$-1.0742e + 00$ $\mp 1.8757e + 01i$	$-1.5061e - 11$ $\pm 2.8731e - 10i$	$-7.7889e - 12$ $\pm 6.8718e - 12i$	-2.0292e+02
11,12	$-1.2172e + 00$ $\mp 2.3587e + 01i$	$1.4187e - 10$ $\pm 2.8776e - 10i$	$-5.4991e - 12$ $\pm 5.3120e - 12i$	-2.0400e+02
13,14	$-1.3234e + 00$ $\mp 2.8317e + 01i$	$2.7987e - 10$ $\pm 1.8675e - 10i$	$-3.6150e - 12$ $\pm 4.8013e - 12i$	-2.0422e+02

Table 3. Data from Prony algorithm for Example 1.

The second phase of Prony fit system and initial condition residues to these modes. An ordering algorithm based on [55] was applied, and the results are given in Table 3.

A plot of the error in dB (column 5 of Table 3) is shown in Figure 4. From this graph a model order of 6 was selected. Figure 5 shows both actual and model output data when the input probing signal described by Table 2 is applied. There is negligible difference in the actual and estimated outputs since there is no noise added to the output of the system.

Example 2: Noisy Case For the second example white-Gaussian noise was added to the measured output. The signal-to-noise ratio of the output signal was 21.5 dB. An initial model order η of 30 was chosen prior to applying the Prony identification technique. After the first phase of Prony was complete, 15 of the 30 modes found were in the 1st or 4th quadrant of the z -plane. The second phase of Prony fit system and initial condition residues to these 15 modes.

A plot of the error in dB similar to Figure 4 is shown in Figure 6. From this

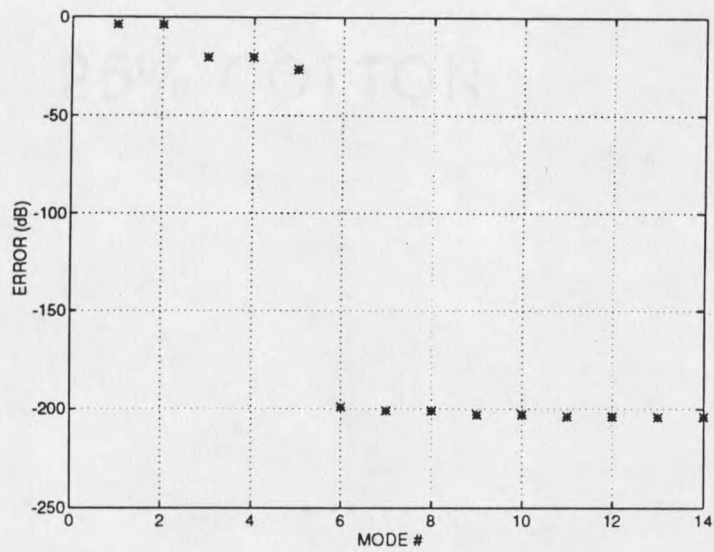


Figure 4. Error in dB for each additional mode set for Example 1.

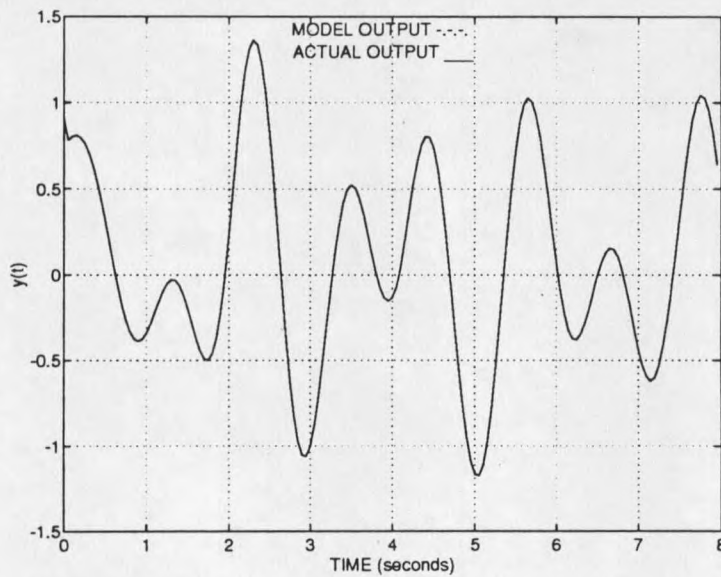


Figure 5. The output for both actual, $y(t)$ and model, $\hat{y}(t)$ for Example 1.

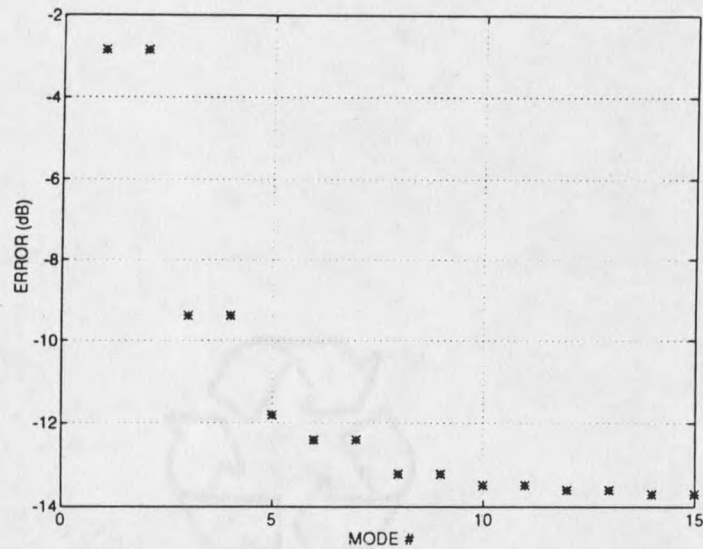


Figure 6. Error in dB for each additional mode set for Example 2.

graph a model order of 7 was selected due to the diminishing return in error with increased model order. Figure 7 shows both actual and model output data when the input probing signal described by Table 2 is applied. The error between the actual and estimated signal is -12.4 dB. Figure 8 shows both actual and model output data without additive noise at the output when the input probing signal described by Table 2 is applied. A plot of the s -domain poles of the actual system and model can be seen in Figure 9. Note that the dominant modes (the less damped modes) have been well identified which is an important feature from a dynamical control point of view. Depending on the type of control being used for system stabilization this model may or may not be adequate.

Example 3: SVA vs. Discrete Prony For a third example we compare *discrete Prony* identification results to those of the SVA method described at the beginning of this chapter which is based on the paper by Moonen, et al., [51]. This

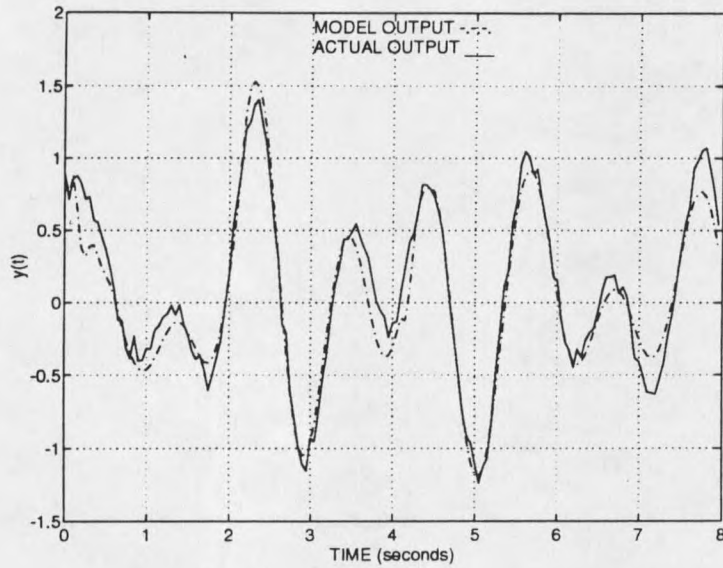


Figure 7. The output for both actual, $y(t)$ and model, $\hat{y}(t)$ for Example 2 with additive output noise.

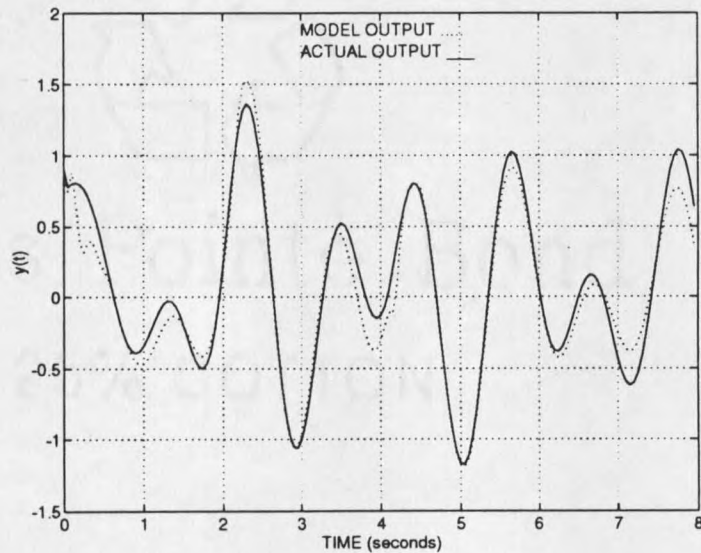


Figure 8. The output for both actual, $y(t)$ and model, $\hat{y}(t)$ for Example 2 with additive output noise removed.

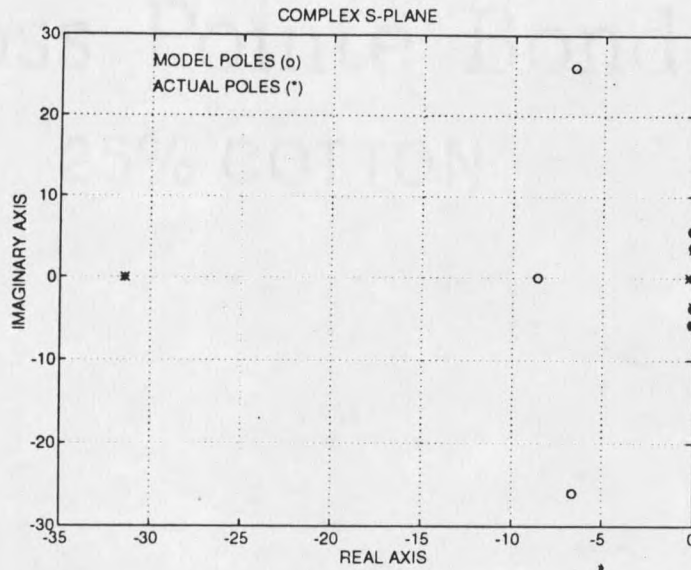


Figure 9. The poles of the s -domain for the actual system and the model for Example 2.

method is referred to as the *Moonen* algorithm. The *Moonen* algorithm was chosen because it parallels the method of *discrete Prony*. The *Moonen* algorithm estimates the states of the system over a time period, whereas *Prony* estimates the modes in the first step and then builds the states of the system prior to fitting the residues to the modes.

A different input probing signal was used in this example for the *discrete Prony* method compared to the previous examples. Here we chose a combination of 14 sinusoidal waves that span the bandwidth of interest, namely, the frequency range from 0 to 3 Hz. The input signal was on for 1 second and then it remained off. The parameter values for (2.27) are given as below and in Table 4:

- $q = 1$ interval
- $m_1 = 14$ input eigenvalues
- $\tau_1 = 1$ second

	$l = 1, 2$	$l = 3, 4$	$l = 5, 6$	$l = 7, 8$	$l = 9, 10$	$l = 11, 12$	$l = 13, 14$
$\mu_{1,l}/(2\pi)$	$\pm 0.25i$	$\pm 0.75i$	$\pm 1.00i$	$\pm 1.25i$	$\pm 1.75i$	$\pm 2i$	$\pm 2.5i$
$c_{1,l}$	$\mp 0.07i$	$\mp 0.07i$	$\mp 0.07i$	$\mp 0.14i$	$\mp 0.14i$	$\mp 0.07i$	$\mp 0.07i$

Table 4. Input drive data for *discrete Prony* of Example 3.

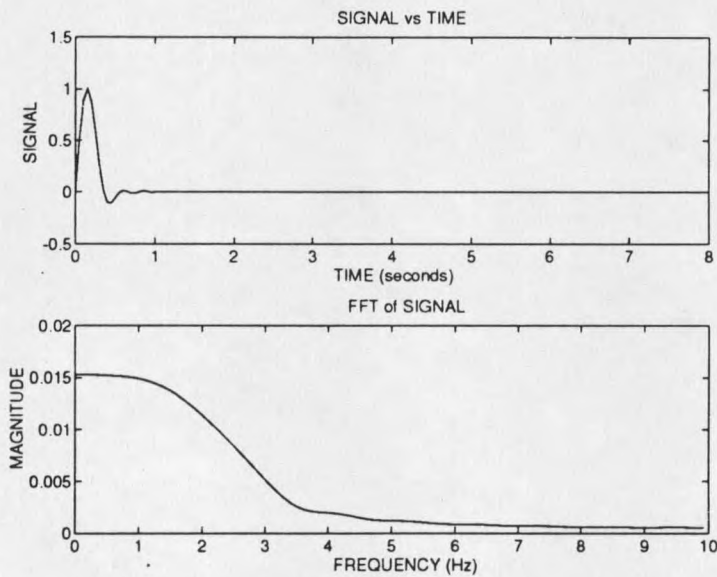


Figure 10. Probing input $u(t)$ and its Fourier transform equivalent for Example 3 using the *discrete Prony* algorithm.

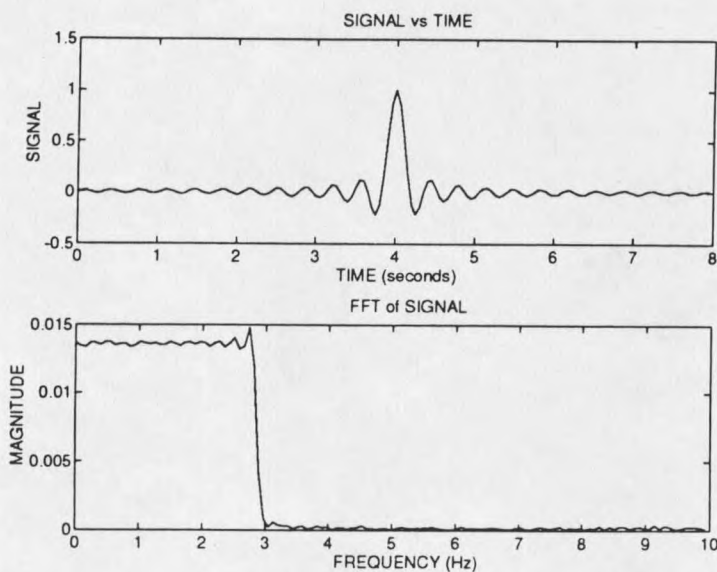


Figure 11. Probing input $u(t)$ and its Fourier transform equivalent for Example 3 using the *Moonen* algorithm.

For the *Moonen* method authors of [51] suggest a pseudo-random input drive signal that sufficiently excites all the modes of the system. Additionally, the signal is assumed to be on for the entire record length. Here we chose to use a SINC type input of (2.55) with energy content that is close to the input used in the *discrete Prony* method (compare the Figures of 10 and 11).

$$u_{\text{sinc}}(t) = m \frac{\sin(2\pi f(t - \Delta t))}{2\pi f(t - \Delta t)} \quad (2.55)$$

where $m = 1$, $f = 18$, and $\Delta t = 4$. Figure 11 shows the SINC type input used. To insure there was no rank deficiency in the Hankel matrix of (2.24) a small amount of normally distributed, zero mean noise was added to the SINC signal of Figure 11.

The *Moonen* algorithm was run for the same case as in Example 1, and the results were very similar to the *discrete Prony* algorithm. Note that there is no user interaction in deciding the model order as can be seen by Figure 12. The algorithm, after computing the rank of the Hankel matrix of (2.24), found the system to be

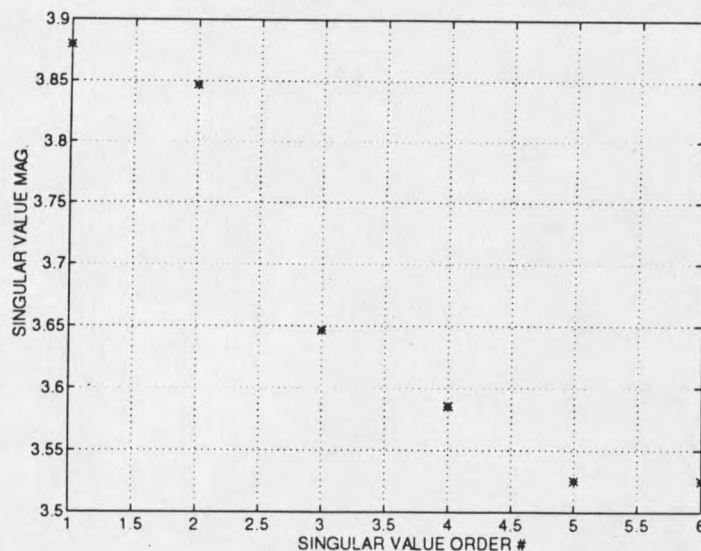


Figure 12. The singular values of the Hankel matrix for Example 3 using the *Moonen* algorithm, no noise case.

of order 6. However, once noise is added to the system, the order selection is not determined by simply computing the rank of this Hankel matrix.

With the input probing signal established for both algorithms the system was subjected to increasing amounts of system noise at a second input, $d(t)$, shown in Figure 2. The noise was normally distributed with zero mean. The variance of the noise input was adjusted to obtain several signal-to-noise ratios at the measured output; these values are given in column one of Table 5. Since the noise is entering at $d(t)$, the effect of the noise on the output is colored due to the dynamics of the system. Note the plot of singular values of the Hankel matrix for the *Moonen* algorithm associated with an SNR of 50 dB in Figure 13. The algorithm shows that the order selected is 23. However, through observation, it appears that the model order may be chosen as 6, which is at the first bend of singular values. This graph of singular values is typical for each of the cases shown in Table 5. From this table it is clear

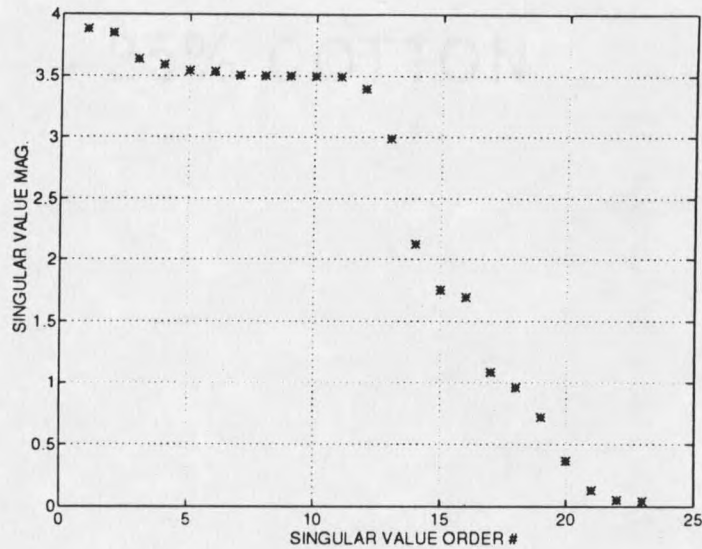


Figure 13. The singular values of the Hankel matrix for Example 3 using the *Moonen* algorithm with 50dB output SNR.

that each method performs relatively the same, where the *discrete Prony* method only does better in the worst noise case. The *Moonen* method has less computation and has less in the way of user interaction.

Noise at Output	<i>Moonen</i> Method		<i>discrete Prony</i> Method	
SNR (dB)	order	error (dB)	order	error (dB)
∞	6	-260.00	6	-199.00
50	6	-55.64	6	-30.85
30	6	-28.73	6	-27.87
20	6	-22.12	6	-21.38
10	6	-6.89	6	-10.85

Table 5. Example 3 error data for noise applied at $d(t)$.

Example 4: One Machine/Infinite Bus Power System As a final example, we consider a power system consisting of one machine, a transmission line and an infinite bus (refer to Figure 14). The infinite bus is an approximation to a large

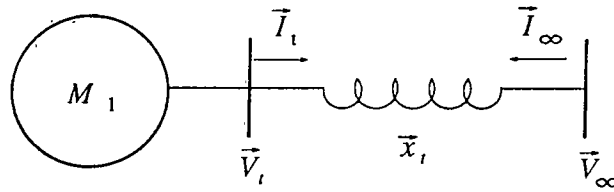


Figure 14. One-machine/infinite-bus power system diagram.

power grid connected to the one machine through a transmission line represented by \vec{x}_t . The per unit value of the infinite bus voltage is $1\angle 0^\circ$ and the per unit value of the injected current of the infinite bus is the negative of \vec{I}_t . In this example we use *discrete Prony* identification to obtain a low order model of the system for control purposes. The ultimate goal is to control speed deviation of the machine following a transmission line fault. This is done by affecting the field voltage of the synchronous machine.

Assuming the system remains in quasi steady-state we are able to write a set of algebraic equations describing the machine bus voltage and the current injected into the transmission line. A set of ordinary differential equations (ODE's) is used to describe the dynamics of the synchronous machine. The algebraic and differential equations are correlated through the so-called D-Q (Direct-Quadrature) axis relations. More detail on these equations is provided in Appendix A. The order of the set of ODE's is 4. The sampling period of the system is set at $T = 0.05$ seconds. The input probing signal for *discrete Prony* identification was a single pulse of amplitude 1 and duration 0.05 seconds and was applied at the reference input to the exciter. The exciter unit is a first-order low-pass filter with gain of 10 and a time-constant of 0.04 seconds. The exciter output is applied to the field voltage input, E_f , of the synchronous machine. The input to the power system stabilizer (PSS) unit was taken as the the speed deviation of the machine. A model of the system using *discrete Prony*

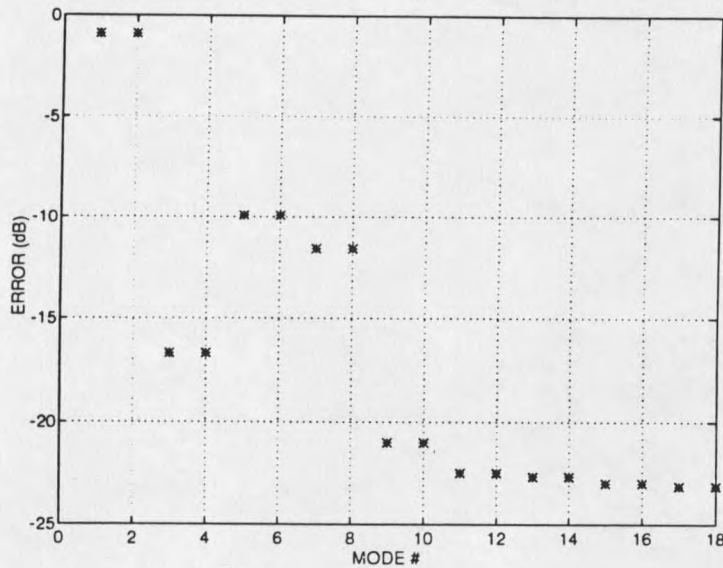


Figure 15. Residue ordering for example 4.

Eigenvalues		Residues	
-1.4056e+00	-1.7651e+00i	-2.3091e+00	+1.8099e+00i
-1.4056e+00	+1.7651e+00i	-2.3091e+00	-1.8099e+00i
-2.9920e-01	+7.2809e+00i	1.8320e+00	+1.1226e+00i
-2.9920e-01	-7.2809e+00i	1.8320e+00	-1.1226e+00i

Table 6. Final model for Example 4.

used the single pulse described above and the speed deviation of the machine as the input/output data. In the first phase of *discrete Prony* identification, 21 eigenvalues were identified. Of these 21, 18 were used in the second stage for residue fitting. A plot of the ordering by the residue method is shown in Figure 15. A model order of 4 was chosen (see Table 6 for the discrete model eigenvalues and residues) with an error in fitted to actual data of -16.7 dB. Using the 4th-order model of Table 6, an LQ gain of

$$K = -[4.8163 \ 2.7961 \ 0.64204 \ -1.4312]$$

was computed for the PSS unit. For state-estimation, a Kalman observer was used (details on the Kalman observer equations are given in the section containing the servo example of Chapter 4). For a detailed diagram of the control scheme, see Figure 16. The disturbance on the transmission line reactance was a change from

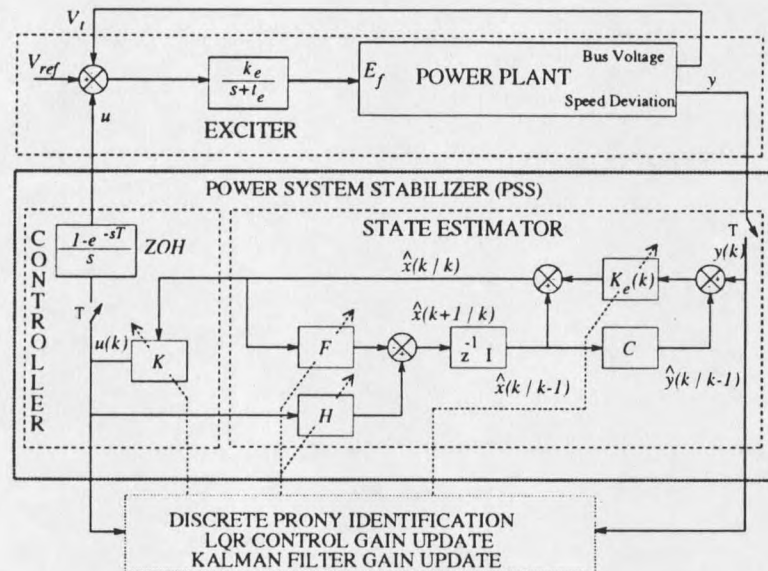


Figure 16. Detailed diagram of control scheme for Example 4.

$\vec{x}_t = j0.2 \text{ p.u.}$ to $\vec{x}_t = j0.35 \text{ p.u.}$ from time $t = 1$ second to $t = 2$ seconds. The results of two simulations are given in Figure 17 where the output signal $y(t)$ is the speed deviation of the machine. The first simulation is for the open-loop case, whereas the second simulation is for the LQG state-feedback case. The value for the LQG input weighting scalar R was chosen to be 10. As shown in Figure 17, the LQG approach using the *discrete Prony* model does improve the damping of the transient condition.

Discussion of Results

A review of various identification methods is given at the start of the chapter. The methods reviewed are based on autoregressive and state-space models. Characteristics

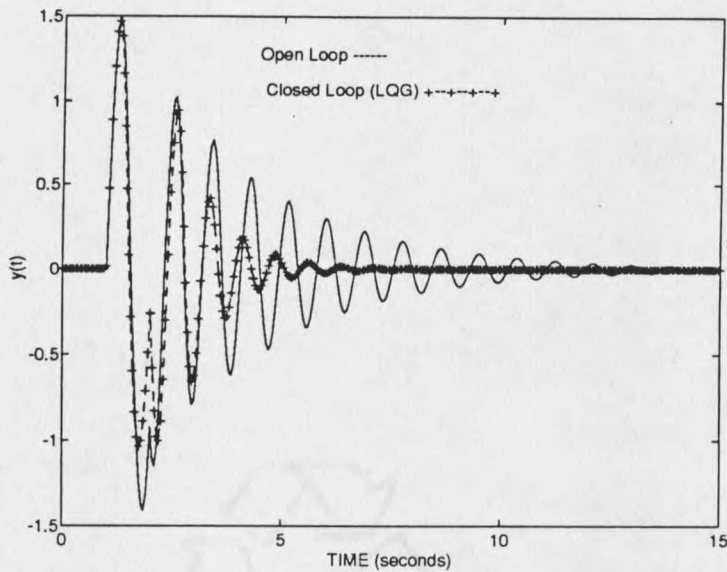


Figure 17. Transient simulation of example 4: Open loop vs. LQG.

of each method were discussed to establish a baseline for the new method developed in this chapter. The method of this chapter is classified as a Prony method because it has two main phases, paralleling the original Prony signal analysis method, in which eigenvalue estimates are generated in the first phase, and residue estimates are calculated in the second phase. Both phases involve linear least-squares solutions that can be obtained with high accuracy using singular value decomposition techniques. The detailed steps used in the two Prony phases of this chapter differ considerably from those of previous Prony-based methods because of the sampled-and-held nature of the input signal. An interesting feature of including the sample-and-hold on the input is that the resulting second Prony phase is actually simplified from the corresponding second Prony phase of [20].

The *discrete Prony* method is for single input/single output systems. The AR methods have this same limitation as opposed to the state-space methods which can handle the multi-input/multi-output case. One feature that is not dealt with in the

AR method and some of the state-space methods is that of establishing an estimate of initial conditions. The state-space method based on SVA does allow for the estimation of initial states of the system. The striking difference of the Prony method from those reviewed is the fact that modes of the system are estimated first. The user may be able to use prior knowledge of the system modes to eliminate extraneous modes from the set. This feature allows for reduced numerical calculations and potential for more accurate residue fitting. The final feature of the *discrete Prony* method is the use of a generalized class of input probing signals that are sampled and held. Prior to being sampled and held, the input signal is piecewise continuous and is characterized by input eigenvalues and input residues between points of discontinuity. The sample period T is the same as that used to collect the sampled system input and output data, which lends itself well to digitally controlled systems. By appropriate selection of the input signal, its energy can be allocated to particular frequency ranges of interest with regard to transfer function identification. Most of the other methods utilize a pseudo-random input signal that essentially has much of its energy at frequency ranges that are not of interest. This type of signal will often not adequately excite those modes that are of interest.

The examples show that with the addition of measured output noise, the approach developed in this chapter can generate fairly good estimates of initial condition residues, transfer function residues, and system eigenvalues. Example 3 shows that the *discrete Prony* method performs relatively well under colored noise environments as compared with other methods. While the effects of system noise on the method presented here remains to be analytically examined, there is a foundation of previous work (e.g., [59, 7, 10, 11, 12, 60, 13]) to build on.

The last example demonstrated the *discrete Prony* identification use in power system stabilization (damping). A low-order model was obtained and used for LQG

state-feedback control. The LQG control based on the *discrete Prony* identified model provided significant damping. In practice, it was found that higher-order models obtained from *discrete Prony* identification were more difficult to utilize in this non-adaptive LQG state-feedback configuration.

CHAPTER 3

SET-MEMBERSHIP APPROACH TO CONTROL DESIGN

In the previous chapter we developed an identification method for digitally controlled systems. Traditionally, the problem of system identification and control design is formulated in an entirely stochastic framework in which the system and its parameters are described by stochastic models. Although the development in Chapter 2 was not formulated in a stochastic framework, a salient feature is that the control input can be easily constructed such that specific frequency ranges of interest are excited, which gives it the ability to overcome (compensate for) the effects of noise in the system. In the ideal case, it is assumed that there exist parameters that exactly describe the true system, which is essentially what many identification schemes assume. This is the case for the *discrete Prony* method, and even though the type of input used can compensate for effects of noise on the estimated model there will always be uncertainty in the parameters estimated.

Once a model is determined one then tries to find a controller which minimizes the expected value of a loss function. This is known as the dual-control problem. A heuristic approach to solving this problem is the traditional adaptive control system in which a model with unknown parameters is assumed for the system. Parameter estimates are obtained recursively in real time, and the controller is designed as if the parameter estimates were in fact the correct parameters for describing the plant. This is known as the *certainty equivalence principle*. Even in the ideal case, the transient errors between the identified model and the true system can be large enough to lead to significant reduction in system performance.

To overcome these shortcomings, a *set-membership approach* to control design is suggested in [36]. The idea of set-membership was first introduced by Fogel [61]. The concept is based on the idea of first estimating a parameter set which, in the ideal case, contains the true parameters of the system. Let this membership set be represented by \mathcal{M} . A control scheme based on this model set is then proposed. Note, the control scheme assumes that each plant within the model set as described by the parameter set estimate is equally likely to be the true plant. Therefore, the controller, if it exists, must stabilize all plants within the membership set \mathcal{M} and as such is considered *robust*. A diagram of such an identification/control scheme is depicted in Figure 18.

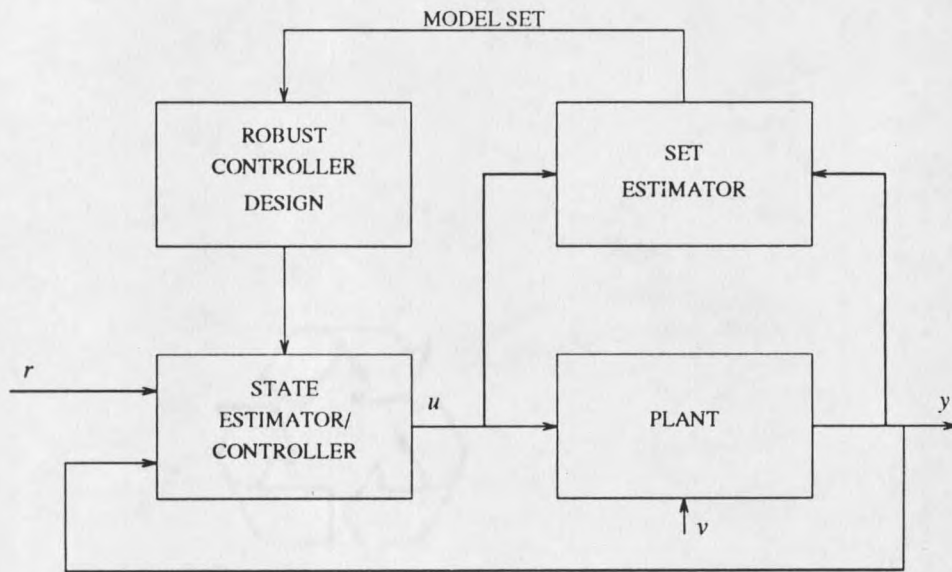


Figure 18. Set-membership adaptive control scheme diagram.

Thus, unlike traditional adaptive control schemes, where parameters are estimated from input/output data and assumed to be equivalent to the true parameters, the set-membership approach, in a sense, selects the worst-case set of parameters from the membership set for the design of the optimal control.

Before describing any particular control strategy for the set-membership ap-

proach we will describe some identification methods that produce membership sets.

Ellipsoid Set Estimation

Two methods of set membership identification are described, each producing a set of real-valued parameters of dimension n that are described by a bounded hyper-ellipsoid in the space $\mathbb{R}^{n \times n}$. The first method of identification assumes no models of uncertainty and arrives at an ellipsoid set which is directly affected by an assumed known bound on the disturbance/noise that acts on the system. The second method of identification assumes a model of non-parametric uncertainty in the model of the system and uses an identification scheme that produces an ellipsoid set of parameters. As expected, this set is directly affected by the model of uncertainty assumed for the system.

Before continuing, consider the following definition of an ellipsoid set.

$$\Omega = \{ \theta : (\theta - \theta_0)^T \Gamma (\theta - \theta_0) \leq 1, \Gamma = \Gamma^T > 0 \}.$$

Geometrically, this ellipsoid set has its center at θ_0 , and the matrix Γ gives its size and orientation; i.e., the square roots of the reciprocals of the eigenvalues of Γ are the lengths of the semi-axes, and the eigenvectors of Γ give their direction.

Disturbance/Noise Induced Ellipsoid

Cheung, et al., [62], have developed what they refer to as the *Optimal Volume Ellipsoid* algorithm (OVE). The algorithm is recursive and is derived for set estimation of a SISO linear time-invariant system with bounded noise. Cast in a recursive framework, where a minimal volume ellipsoid results at each recursion, the algorithm extends a result due to Khachian [63] in which a technique was developed to solve a class of linear programming problems (see [64] for extensions of Khachian's results).

Consider the the SISO ARX model

$$\begin{aligned} y(k) &= -\sum_{i=1}^{n_a} a_i y(k-i) + \sum_{j=1}^{n_b} b_j u(k-j) + \nu(k) \\ &= \theta^T \phi(k) + \nu(k) \end{aligned} \quad (3.1)$$

where $\theta^T = [a_1, \dots, a_{n_a}, b_1, \dots, b_{n_b}]$ is the parameter vector to be estimated; the regression vector containing the past input and output values is given by $\phi(k) = [-y(k-1), \dots, -y(k-n_a), u(k-1), \dots, u(k-n_b)]^T$. The term $\nu(k)$ is a sequence of bounded disturbances/noise corrupting the system output with $|\nu(k)| \leq \gamma$ for all $k \geq 0$. It is assumed that the number of parameters is known a priori as well as the bound on the disturbance; thus we are given n_a , n_b , and γ . The total number of parameters is $n = n_a + n_b$.

Let $\mathcal{F} \in \mathbb{R}^n$ be a set such that all $\theta \in \mathcal{F}$ are feasible parameter estimates of the plant which are consistent with the measurements. That is

$$\mathcal{F} = \{\theta : |y(k) - \theta^T \phi(k)| \leq \gamma, \quad k = 0, \dots, N\}. \quad (3.2)$$

The membership \mathcal{M} is defined by (3.2). The problem of parameter set estimation is to find \mathcal{F} explicitly in the parameter space. In general, \mathcal{F} is an irregular convex set; therefore, the algorithm finds the smallest ellipsoid that contains the set \mathcal{F} where the hyper-volume of an ellipsoid is used to measure "smallness". Consistency of measurement provides a pair of constraints which establishes the framework for a minimal volume ellipsoid. The first constraint comes directly from (3.2) and the second is in terms of the predicted set \mathcal{F}_{k+1} which are given by

$$\begin{aligned} \text{constraint1} & : & |y(k) - \theta^T \phi(k)| & \leq \gamma \\ \text{constraint2} & : & \mathcal{F}_{k+1} & = \{\theta : |y(k+1) - \theta^T \phi(k+1)| \leq \gamma\}. \end{aligned}$$

Geometrically, \mathcal{F}_{k+1} is the region between two parallel hyper-planes defined by *constraint 2*. The set estimation problem is then stated as: Given an ellipsoid Ω_k , find

another ellipsoid Ω_{k+1} with minimal volume, such that Ω_{k+1} contains $\Omega_k \cap \mathcal{F}_{k+1}$, for $k = 0, \dots, N$, where N is the number of data records. Mathematically, the optimization problem becomes

$$\min\{\text{vol}(\Omega_{k+1}) : \Omega_{k+1} \supset \Omega_k \cap \mathcal{F}_{k+1}\}.$$

The authors of [62] define Ω_k and Ω_{k+1} as

$$\Omega_k \triangleq \{\theta : (\theta - \theta_k)^T \Gamma_k (\theta - \theta_k) \leq 1; \theta \in \mathbb{R}^n\} \quad (3.3)$$

and

$$\Omega_{k+1} \triangleq \{\theta : (\theta - \theta_{k+1})^T \Gamma_{k+1} (\theta - \theta_{k+1}) \leq 1; \theta \in \mathbb{R}^n\},$$

where Γ is symmetric and positive definite and θ_k is the center estimate of the ellipsoid at time k . The algorithm amounts to recursively estimating θ_k and Γ_k at each time instant k . The algorithm is initialized by assuming that θ_0 and Γ_0 are such that the ellipsoid Ω_0 includes the true parameters of the system. This is accomplished by selecting the eigenvalues of Γ_0 such that Ω_0 is sufficiently large. For details and attributes of the OVE algorithm see [62] and references therein.

Non-parametric Uncertainty Induced Ellipsoid

The method of identification outlined below is found in [36]. The model set \mathcal{M} is defined as follows:

$$\mathcal{M} \triangleq \{y = Gu : G \in \mathcal{G}\} \quad (3.4)$$

and

$$\mathcal{G} \triangleq \{G_\theta(1 + \Delta_G W_G) : \theta \in \Omega_{\text{prior}}, \|\Delta_G\|_{H_\infty} \leq 1\}, \quad (3.5)$$

where $G_\theta(z)$ is a parametric z-transform transfer function with parameters $\theta \in \Omega_{\text{prior}}$, referred to as the prior parameter set. The system $\Delta_G W_G$ is referred to as the multiplicative non-parametric uncertainty, which is a dynamic uncertainty described

by an uncertain but unity bounded stable transfer function $\Delta_G(z)$ and a known stable transfer function $W_G(z)$. Having knowledge of W_G is precisely the assumption made in robust control design, e.g., [28]. The H_∞ norm for z -transform functions is defined as

$$\|G\|_{H_\infty} \triangleq \sup_{|\omega| \leq \pi} |G(e^{j\omega})|.$$

Solving for Δ_G in (3.5) in terms of G and θ , we get

$$\Delta_G(z) = \frac{G(z) - G_\theta(z)}{W_G(z)G_\theta(z)}.$$

We define

$$\Omega^* \triangleq \left\{ \theta : \left\| \frac{G(z) - G_\theta(z)}{W_G(z)G_\theta(z)} \right\|_{H_\infty} \leq 1 \right\}$$

and refer to Ω^* as the true-plant set because it does not depend on the data set but rather on the true but unknown system G . Since the decomposition of G into G_θ and Δ_G is not unique, it is not possible to consider a "true" parameter value for the plant. Therefore, we want to find a set estimate,

$$\hat{\Omega} \triangleq \hat{\Omega}^* \cap \Theta_{prior},$$

where $\hat{\Omega}^*$ is an estimate of Ω^* . As a result, $\hat{\Omega}$, is a set estimate of *all* possible parameter values consistent with the assumption that the true system G is in the model set \mathcal{G} . We further characterize the parametric transfer function $G_\theta(z)$ by using the standard ARX form of (3.1).

Before we state a main result of [36] we must define several terms. Let $\mathcal{E}_k(\cdot)$ be defined as the sample-mean operator,

$$\mathcal{E}_k(x) \triangleq \frac{1}{k} \sum_{j=1}^k x(j), \quad (3.6)$$

and $\|x\|_{k2}$ be defined as the truncated l_2 -norm of a sequence,

$$\|x\|_{k2} \triangleq \left(\sum_{j=1}^k x(j)^2 \right)^{\frac{1}{2}}.$$

Hence,

$$\frac{1}{k} \|x\|_{k2}^2 = \frac{1}{k} \sum_{j=1}^k x(j)^2 = \mathcal{E}_k(xx)$$

where x is a scalar value. Next, we define the following regression vectors:

$$\begin{aligned} \phi_y &\triangleq [-z^{-1}y \ \dots \ -z^{-n_a}y]^T, \\ \phi_u &\triangleq [-z^{-1}u \ \dots \ -z^{-n_b}u]^T, \\ \phi &\triangleq \begin{bmatrix} \phi_y \\ \phi_u \end{bmatrix}, \\ \alpha_k &\triangleq \mathcal{E}_k(yy), \\ \beta_k &\triangleq \mathcal{E}_k(\phi y), \\ \Gamma_k &\triangleq \mathcal{E}_k(\phi\phi^T) - \begin{bmatrix} 0 & 0 \\ 0 & \mathcal{E}_k((W_G\phi_u)(W_G\phi_u)^T) \end{bmatrix}, \end{aligned}$$

where $\alpha_k \in \mathbb{R}$, $\beta_k \in \mathbb{R}^\eta$, and $\Gamma_k \in \mathbb{R}^{\eta \times \eta}$, with $\eta = n_a + n_b$. By the definition of \mathcal{E}_k given in (3.6) we see that $\mathcal{E}_k(yy)$ is computed by first performing the multiplication out term-by-term before taking the sample mean. To compute $\mathcal{E}_k(\phi\phi^T)$, multiply ϕ and ϕ^T to produce a matrix of sequences, then take the sample mean of each element. Finally, by letting $G_\theta(z) = B_\theta(z)/A_\theta(z)$ where

$$\begin{aligned} B_\theta(z) &= b_1z^{-1} + \dots + b_{n_b}z^{-n_b}, \\ A_\theta(z) &= 1 + a_1z^{-1} + \dots + a_{n_a}z^{-n_a} \end{aligned}$$

we can state the primary result of Lau's and give the solution for estimation of Ω^* .

Theorem 3.1 (Lau [36]) *Suppose the measured data $\{y, u : j = 1, \dots, N\}$ is generated from $y = Gw$ as defined in (3.4). Then the following holds:*

$$\Omega^* \subseteq \Omega[N] \subseteq \Omega_k, \quad \forall k \in [1, N], \quad \forall N \in \mathbb{N}$$

where $\Omega[N]$ and Ω_k are given by,

$$\begin{aligned} \Omega_k &\triangleq \{\theta : \|A_\theta y - B_\theta u\|_{k2} \leq \|W_G B_\theta u\|_{k2}\} \\ \Omega[N] &\triangleq \bigcap_{k=1}^N \Omega_k. \end{aligned}$$

An estimate of the parameters can now be obtained from Ω_k since Ω^* is a subset of Ω_k . Lau goes on to show that:

I. Ω_k can be expressed in quadratic form as

$$\Omega_k = \{ \theta : \theta^T \Gamma_k \theta - 2\beta_k^T \theta + \alpha_k \leq 0 \}.$$

II. If Γ_k^{-1} exists, then

$$\Omega_k = \{ \theta : (\theta - \hat{\theta}_k)^T \Gamma_k (\theta - \hat{\theta}_k) \leq V_k \}, \quad (3.7)$$

where

$$\hat{\theta}_k = \Gamma_k^{-1} \beta_k.$$

$$V_k = \beta_k^T \Gamma_k^{-1} \beta_k - \alpha_k.$$

Assuming V_k is nonzero we can divide through the inequality of (3.7) by V_k and obtain an expression similar to the ellipsoid expression found in (3.3). Note, $\hat{\theta}_k$ is identical to the ordinary least-squares estimate when $W_G = 0$ (no nonparametric dynamics), i.e.,

$$\theta_{LS} = (\mathcal{E}_k(\phi\phi^T))^{-1} \mathcal{E}_k(\phi y).$$

This gives the set estimate Ω_k a nice geometric interpretation because it is centered at the estimate one usually gets by ignoring the nonparametric uncertainty and applying least-squares estimation. The center of the ellipsoid estimate of Cheung does not necessarily have as its center the least-squares estimate. For ellipsoid uncertainty algorithms similar to Cheung that have the least-squares estimate as their center see [65].

Linear Quadratic Regulator

This section includes a tutorial on linear quadratic regulator (LQR) control theory. We first describe the standard cost function that is commonly used in control theory for the continuous time system. We introduce the algebraic Riccati equation and its role in optimal state feedback control. Lastly, the discrete counterpart to the continuous time solution is given. Following this section we combine the ideas here and in the previous sections to state a set-membership control method in the form of a minimaximization problem.

Continuous-Time LQR

A common objective for the feedback regulation problem is to minimize the energy of the output signal over time. This is accomplished by determining a control signal $\mathbf{u}(t)$ that optimally minimizes the integral of $\mathbf{y}(t)^T \mathbf{y}(t)$ over time. The control signal that accomplishes this is referred to as the optimal control and is represented by $\mathbf{u}^*(t)$. However, without any penalty on the magnitude of the control signal $\mathbf{u}(t)$, it is possible that $\mathbf{u}(t)$ may reach amplitudes that are not acceptable in the actual system. To introduce trade-off between magnitudes of $\mathbf{u}(t)$ and $\mathbf{y}(t)$ we place weights on both $\mathbf{u}(t)$ and $\mathbf{y}(t)$ and construct what is commonly referred to as the LQR cost function which when minimized over time gives the optimal LQR state-feedback gain K_{LQR} . Essentially, the objective is to keep the magnitude of the output $\mathbf{y}(t)$ small while not using too much control effort.

For the remainder of this and other chapters, K will be considered the same as K_{LQR} unless otherwise noted. Following is a summary of the standard LQR results. Given a linear time-invariant system represented by (2.7) the quadratic regulator problem is to find a control $\mathbf{u}(t)$ to minimize the cost

$$J = \int_0^{\infty} [\mathbf{u}(t)^T R \mathbf{u}(t) + \mathbf{x}(t)^T Q \mathbf{x}(t)] dt. \quad (3.8)$$

Note that J is an explicit function of $\mathbf{y}(t)$ under the condition that $\mathbf{y}(t) = C\mathbf{x}(t)$ and $Q = C^T C$. In general, the weighting matrix Q should be positive-semidefinite, and R should be positive-definite. Under the assumptions that (A, B) is stabilizable and $(Q^{\frac{1}{2}}, A) = (C, A)$ is detectable, this problem has the well-known solution [66]

$$\mathbf{u}^*(t) = -K\mathbf{x}(t), \quad (3.9)$$

where the state-feedback gain K is given by

$$K = R^{-1}B^T P \quad (3.10)$$

and P denotes the unique positive-definite solution of the algebraic Riccati equation

$$A^T P + PA - PBR^{-1}B^T P + Q = 0. \quad (3.11)$$

With the optimal control $\mathbf{u}^*(t)$, the LQR cost is

$$J = \mathbf{x}(0)^T P \mathbf{x}(0).$$

Since the close-loop system must be stable for the cost to be finite, there exists a positive-definite matrix L which solves the associated Lyapunov equation,

$$(A - BK)^T L + L(A - BK) + S = 0 \quad (3.12)$$

for any positive-semidefinite symmetric matrix S . In particular, if $S = \mathbf{x}(0)\mathbf{x}(0)^T$, then

$$L = \int_0^\infty [e^{(A-BK)^T t} S e^{(A-BK)t}] dt, \quad (3.13)$$

which is sometimes referred to as the controllability grammian [29]. Finally, the stable closed-loop solution of (2.7) for the control gain given in (3.10) is simply

$$\mathbf{x}(t) = e^{(A-BK)t} \mathbf{x}(0).$$

Discrete-Time LQR

Given the discrete-time linear system of (2.10) and (2.11) the problem is to find $\mathbf{u}(k)$ so that

$$J = \sum_{k=0}^N [\mathbf{x}(k)^T Q \mathbf{x}(k) + \mathbf{u}(k)^T R \mathbf{u}(k)] \quad (3.14)$$

is minimized. The optimal solution [46] is given by the state-feedback

$$\mathbf{u}^*(k) = -K(k)\mathbf{x}(k), \quad (3.15)$$

where the state-feedback gain K is a time-varying gain given by

$$K(k) = [R + H^T P(k+1)H]^{-1} H^T P(k+1)F \quad (3.16)$$

and P obeys the discrete Riccati equation

$$P(k) = F^T P(k+1)F - F^T P(k+1)H [R + H^T P(k+1)H]^{-1} H^T P(k+1)F + Q \quad (3.17)$$

with boundary condition

$$P(N) = Q.$$

Note that even though $K(k)$ is time-varying, it can be precomputed as long as the length N is known. This is because K is not a function of the initial state $\mathbf{x}(0)$. The LQR cost for the optimal control is

$$J = \mathbf{x}(0)^T P(0)\mathbf{x}(0).$$

For the infinite-horizon problem, where $N \rightarrow \infty$, the constant gain solution is the optimum. In steady-state, $P(k)$ becomes $P(k+1)$ and the Riccati equation reduces to

$$P_\infty = F^T P_\infty F - F^T P_\infty H [R + H^T P_\infty H]^{-1} H^T P_\infty F + Q. \quad (3.18)$$

The optimal control is

$$\mathbf{u}(k) = -K_\infty \mathbf{x}(k), \quad (3.19)$$

where

$$K_\infty = [R + H^T P_\infty H]^{-1} H^T P_\infty F. \quad (3.20)$$

The cost associated with this control law is

$$J_\infty = \mathbf{x}(0)^T P_\infty \mathbf{x}(0).$$

Minimaximization Problems

We now state the general set-membership approach to control design. Let us first consider the continuous time system of (2.7) and (2.8). We assume that the plant to be controlled is known to belong to a set \mathcal{M} as described by Ω of (3.3). Specifically, this means $\theta \in \Omega$, where θ is a parameter vector that parameterizes the plant. We want to find a control $\mathbf{u} : \mathbb{R}_+ \mapsto \mathbb{R}^n$ that solves the following minimax problem:

$$\min_{\mathbf{u}} \max_{\theta \in \Omega} J \quad (3.21)$$

where J is the usual quadratic cost given in (3.8). More precisely, the goal is to find a saddle-point (\mathbf{u}^*, θ^*) such that

$$J(\mathbf{u}^*, \theta) \leq J(\mathbf{u}^*, \theta^*) \leq J(\mathbf{u}, \theta^*) \quad \forall \mathbf{u} \text{ and } \theta \in \Omega. \quad (3.22)$$

From a game-theoretic point of view, the first player, $\theta \in \Omega$, attempts to maximize the cost and the second player, $\mathbf{u} \in \mathbb{R}^n$, attempts to minimize the cost. Since no particular form is assumed for the control \mathbf{u} , such as linear state-feedback, the minimization is over all possible \mathbf{u} 's, i.e., all time functions. Note that this same assumption is made initially for the linear quadratic optimal control problem where the plant is known, but the optimal control in that case exhibits the form of linear state-feedback control, (3.9). When this control design is implemented in conjunction

with a set-membership identifier, as described above, a new controller can be designed each time the set estimate, $\widehat{\mathcal{M}}$, is updated.

The minimax problem formulated in [36] is a good example where the first player is a vector θ as defined in (3.3) which describes a parametric uncertainty for the output matrix C of (2.11) and the second player is \mathbf{u} of form shown in (3.9).

Example: Lau

The formulation of the problem is as follows. Consider the strictly proper system ($D = 0$) of (2.7) and (2.8) of an uncertain system \mathcal{M} where A , B and $\mathbf{x}(0) = \mathbf{x}_0$ are given. The elements of $C \in \mathbb{R}^{m_0 \times n_a}$ are in the set Ω defined as:

$$\Omega = \{ \theta : (\theta - \theta_0)^T \Gamma (\theta - \theta_0) \leq 1 \}, \quad (3.23)$$

where Γ is symmetric and positive definite and θ_0 is the center of the ellipsoid. In general, we can take the rows of C , turn them into column vectors and stack them on top of each other to form a $\mathbb{R}^{m_0 n_a}$ column vector \mathbf{c} such that $\theta = \mathbf{c} \in \Omega$, i.e.,

$$C^T = [\mathbf{c}_1 \ \mathbf{c}_2 \ \cdots \ \mathbf{c}_{m_0}] \in \mathbb{R}^{m_0 \times n_a}$$

$$\mathbf{c} = \begin{bmatrix} \mathbf{c}_1 \\ \mathbf{c}_2 \\ \vdots \\ \mathbf{c}_{m_0} \end{bmatrix} \in \mathbb{R}^{m_0 n_a \times 1}.$$

For a given control, $\mathbf{u} : \mathbb{R}_+ \mapsto \mathbb{R}^{m_i}$, and a fixed $\mathbf{c} \in \Omega$, the objective is defined to be

$$J(\mathbf{u}, \mathbf{c}) \triangleq \int_0^\infty [\mathbf{u}(t)^T R \mathbf{u}(t) + \mathbf{y}(t)^T \mathbf{y}(t)] dt \quad (3.24)$$

where $R \in \mathbb{R}^{m_i \times m_i}$ is a known weighting matrix. Equation (3.24) can be obtained from (3.8) with $Q = C^T C$ and $\mathbf{y}(t) = C \mathbf{x}(t)$. We assume that (A, B) is controllable (at least stabilizable) and (C, A) is observable (at least detectable) for all \mathbf{c} in Ω . The robust control problem is to find a control \mathbf{u} that solves the following minimax

problem:

$$\min_{\mathbf{u} \in \mathbb{R}^m} \max_{\mathbf{c} \in \Omega} J(\mathbf{u}, \mathbf{c}). \quad (3.25)$$

Rewriting (3.24) as

$$J(\mathbf{u}, \mathbf{c}) \triangleq \int_0^\infty [\mathbf{u}(t)^T R \mathbf{u}(t) + \mathbf{x}(t)^T C^T C \mathbf{x}(t)] dt \quad (3.26)$$

leads to another interpretation. We can say that we are designing a controller for a set of uncertain plant cost objectives; in contrast, the standard LQR design is to find a controller for fixed weighting matrices, Q and R . In [36] $(\mathbf{u}^*, \mathbf{c}^*)$ is shown to exist such that

$$J(\mathbf{u}^*, \mathbf{c}) \leq J(\mathbf{u}^*, \mathbf{c}^*) \leq J(\mathbf{u}, \mathbf{c}^*) \quad \forall \mathbf{u} \text{ and } \mathbf{c} \in \Omega \quad (3.27)$$

and that the optimal control is actually the state-feedback LQR control of (3.9), i.e., $\mathbf{u}^*(t) = \mathbf{u}_{LQR}(\mathbf{c}^*)$. Lau proves existence of $(\mathbf{u}^*, \mathbf{c}^*)$ by fixed point theory and shows that the solution must reside on the boundary of the ellipse; two methods for finding the saddle-point solution are given. The first method is an iterative fixed-point algorithm for which there are no guarantees of convergence. The second approach is based on linear matrix inequality methods (LMI, see [67]) where the feedback gain K of (3.10) is computed directly. The method is guaranteed to converge to within any arbitrary degree of accuracy to the solution $(\mathbf{u}^*, \mathbf{c}^*)$. For details see [36] and references therein.

Example: Mills

An approach based on the calculus of variation is proposed in [68]. The approach uses a parameter-change norm, σ , which was first proposed in [69]

$$\sigma^2 = \Delta_\theta^T \Sigma^{-2} \Delta_\theta. \quad (3.28)$$

Δ_θ is a vector of plant parameter changes from nominal. Σ is a symmetric weighting matrix, typically a diagonal matrix of standard deviations of the parameters about the

nominal, mean values. A larger element of Σ allows more variation in the corresponding parameter for a given norm σ . The quadratic norm (3.28) therefore has Gaussian interpretation. Physical system uncertainty often closely follows and is modeled with Gaussian distribution.

Of particular interest is a minimax problem proposed in [68] which iteratively determines the worst-case plant and optimal controller for a set of plants defined by the parameter-change norm (3.28). The cost function is given as

$$J = \min_{u_{LQR}} \max_{\Delta\theta(\sigma)} \int_0^{\infty} (\mathbf{x}(t)^t Q \mathbf{x}(t) + \mathbf{u}(t)^T R \mathbf{u}(t)) dt$$

with standard assumptions on Q and R . The parameter-change norm σ is assumed a priori. The procedure first involves the maximization for a given linear quadratic control u_{LQR} over the set of plants related to the equality constraint defined by (3.28). Necessary conditions are provided for achieving a maximization. The maximization procedure is the result of standard methods used in the calculus of variations. After the plant associated with the maximization is determined the procedure continues by computing the optimal LQR feedback control u_{LQR} . The algorithm proceeds until a saddle-point is found. Conditions for obtaining a saddle-point are discussed in [68].

Proposed Minimaximization Problems

While Lau has considered the problem where uncertainty is only in the output matrix C , it is natural to consider the problem where uncertainty in the matrices A and B can be placed in the form of ellipsoidal bounds on the associate parameters. Furthermore, unlike the approach taken in [68], it is worth considering the case where the parameters are allowed to vary over the entire space defined by the ellipsoidal bound. In addition, current *ellipsoid* identification schemes are restricted to SISO systems as seen in [65, 62, 36, 70]. A natural minimax problem to consider then is for the SISO system. Next, we construct the minimax problem for both the continuous time and discrete

time system where the uncertainty in the numerator and denominator parameters is contained in a bounded ellipsoidal domain.

Continuous Plant Consider the strictly proper case of the system of (2.9) (i.e., set $b_{n_b+1} = 0$ and $n_b \leq n_a$) where there is uncertainty in the numerator and denominator parameters. In observable form (2.7) and (2.8) are represented as

$$A \triangleq \begin{bmatrix} 0 & \cdots & 0 & -a_1 \\ \vdots & & & -a_2 \\ I & & & \vdots \\ \vdots & & & -a_{n_a} \end{bmatrix}, \quad B \triangleq \begin{bmatrix} b_1 \\ b_2 \\ \vdots \\ b_{n_b} \\ \mathbf{0}^{(n_a-n_b)} \end{bmatrix}$$

and

$$C \triangleq [0 \ \cdots \ 0 \ 1].$$

Define the parameter set θ_{AB} by

$$\theta_{AB}^T \triangleq [a_1 \ a_2 \ \cdots \ a_{n_a} \ b_1 \ b_2 \ \cdots \ b_{n_b}]^T. \quad (3.29)$$

The parameter uncertainty set in θ_{AB} is defined as follows:

$$\Omega \triangleq \{\theta_{AB} : (\theta_{AB} - \theta_o)^T \Gamma (\theta_{AB} - \theta_o) \leq 1\}, \quad (3.30)$$

where θ_o contains the nominal values of the system parameters defined as

$$\theta_o^T \triangleq [\theta_{o1} \ \theta_{o2} \ \cdots \ \theta_{o\{n_a+n_b\}}] \quad (3.31)$$

and matrix Γ defines the bound and is symmetric and positive definite given by

$$\Gamma \triangleq \begin{bmatrix} \gamma_1 & \gamma_2 & \gamma_3 & \cdots & \gamma_{\eta-1} & \gamma_{\eta} \\ \gamma_2 & \gamma_{\eta+1} & \gamma_{\eta+2} & \cdots & \gamma_{2\eta-2} & \gamma_{2\eta-1} \\ \gamma_3 & \gamma_{\eta+2} & \gamma_{2\eta} & \gamma_{2\eta+1} & \cdots & \vdots \\ \vdots & \vdots & \vdots & \vdots & \ddots & \vdots \\ \gamma_{\eta-1} & \gamma_{2\eta-2} & \cdots & \cdots & \cdots & \vdots \\ \gamma_{\eta} & \gamma_{2\eta-1} & \cdots & \cdots & \cdots & \gamma_{\frac{\eta(\eta+1)}{2}} \end{bmatrix}, \quad (3.32)$$

where $\eta \triangleq n_a + n_b$.

The problem is to find a control signal $u(t)$ that stabilizes $G(s)$ of (2.9) for all $\theta_{AB} \in \Omega$ and is optimum in the sense of the minimaximization of the quadratic cost function

$$J(u, \theta_{AB}) \triangleq \int_0^{\infty} [u(t)^T R u(t) + y^2(t)] dt \quad (3.33)$$

where $R > 0$ is a known weighting scalar. In general, the existence of such an optimal control signal will be dependent on the size of Γ and the stabilizability of the system (2.9) over the parameter space $\theta_{AB} \in \Omega$. From dynamic game theory [71], $J(u^*, \theta_{AB}^*)$ is optimum if and only if

$$J(u^*, \theta_{AB}) \leq J(u^*, \theta_{AB}^*) \leq J(u, \theta_{AB}^*) \quad (3.34)$$

for all $u : \mathbb{R}_+ \rightarrow \mathbb{R}$ and $\theta_{AB} \in \Omega$. Note that the type of control has not been established and therefore can either be linear or nonlinear. However, from LQR control theory, the second inequality in (3.34) is true if and only if

$$u^* = u_{LQR}(\theta_{AB}^*),$$

where $u_{LQR}(\theta_{AB}^*)$ denotes the LQR control designed for the plant with $\theta_{AB} = \theta_{AB}^* \in \Omega$. Thus, if a saddle point exists, the type of control implemented must be of the state feedback form given by (3.9).

Discrete Plant The discrete counterpart to the continuous time SISO system is now stated. If the sampling rate is given by T and $z \triangleq e^{Ts}$ the pulse-transfer function is simply given by

$$G(z) = \frac{b_1 z^{-1} + \dots + b_{n_b} z^{-n_b}}{1 + a_1 z^{-1} + \dots + a_{n_a} z^{-n_a}} \quad (3.35)$$

where $n_b \leq n_a$. In observable form (2.10) and (2.11) are represented as

$$F \triangleq \begin{bmatrix} 0 & \cdots & 0 & -a_{n_a} \\ \vdots & & & -a_{n_a-1} \\ & I & & \vdots \\ & & & -a_1 \end{bmatrix}, \quad H \triangleq \begin{bmatrix} 0^{(n_a-n_b)} \\ b_{n_b} \\ b_{n_b-1} \\ \vdots \\ b_1 \end{bmatrix}$$

and

$$C \triangleq [0 \ \cdots \ 0 \ 1].$$

It is clear that the a_i 's and b_i 's of (3.35) differ from those of the continuous case of (3.29). However, the parameters in a_i and b_i can be assigned in the same way as in the continuous case, as also can the parameter uncertainty set Ω (3.30). Replacing the subscripts AB with FH we obtain the parameter uncertainty set in θ_{FG} as follows:

$$\Omega \triangleq \{\theta_{FH} : (\theta_{FH} - \theta_o)^T \Gamma (\theta_{FH} - \theta_o) \leq 1\}, \quad (3.36)$$

where θ_o contains the nominal values of the system parameters. The nominal parameter vector and the matrix Γ are defined in the same way as in the continuous time case.

The problem is to find a control signal $u(k)$ that stabilizes $G(z)$ of (3.35) for all $\theta_{FH} \in \Omega$ and is optimum in the sense of the minimaximization of the quadratic cost function

$$J(u, \theta_{FH}) \triangleq \sum_{k=0}^{\infty} [u(k)^T R u(k) + y^2(k)] \quad (3.37)$$

where $R > 0$ is a known weighting scalar.

Discussion of Results

This chapter has served to introduce two minimaximization problems. The review of linear quadratic control theory provided the necessary tools to establish the statement of the problem. Motivation for these problems is primarily due to the efforts of Lau,

Fogel and Cheung [32, 61, 62] in the area of system identification and the efforts of Lau and Mills [72, 68] in the area of set-membership control. From standard results in linear quadratic control theory we see that, in order to determine the saddle point solution, the control strategy for the minimaximization problem must be LQR linear state-feedback. The problems are different from those of Lau and Mills in that the uncertain parameters are the parameters of the state-space matrices A and B (or F and H) and are allowed to vary within a bounded ellipsoidal domain. The ellipsoidal domain is determined through identification schemes similar to the method of Cheung [62]. The following chapter proposes a fixed-point iterative algorithm to find the desired saddle-point solution. The iterative solutions for the continuous and the discrete time systems are very similar.

CHAPTER 4

MINIMAXIMIZATION FOR SINGLE-INPUT SINGLE-OUTPUT SYSTEMS

In this chapter we derive an iterative algorithm for finding a saddle-point to the minimax problem developed in the previous chapter. Both the continuous-time and discrete-time SISO plants are considered where the system parameters are allowed to vary over the entire ellipsoidal domain defined by (3.30) and (3.36), respectively.

Continuous-Time System Problem Statement

The system is described by (2.7)-(2.9) where we set $b_{n_b+1} = 0$ and $n_b \leq n_a$, and by (3.29) and (3.30). As discussed in Chapter 3, the form of the control that is of interest here is linear state feedback

$$u(t) = -K\mathbf{x}(t).$$

The set of stabilizing controllers is defined by

$$\mathcal{K} \triangleq \{K : K \text{ stabilizes } G(s) \forall \theta_{AB} \in \Omega\}.$$

Those cases where \mathcal{K} is nonempty are of interest.

Statement of Problem: Find a controller $K^* \in \mathcal{K}$ that stabilizes $G(s) \forall \theta_{AB} \in \Omega$ and is optimum in the sense of the minimaximization of the quadratic cost function

$$J(K, \theta_{AB}) = \int_0^{\infty} \mathbf{x}^T(t)(K^T R K + C^T C)\mathbf{x}(t)dt, \quad (4.1)$$

where R is symmetric and positive definite, and $\mathbf{x}(t) = e^{(A-BK)t}\mathbf{x}(0)$. Since the system is SISO, $R \in \mathbb{R}$ is scalar and must be greater than 0. This problem is equivalent

to finding a saddle point solution. Note that (4.1) is equivalent to (3.8) under the condition that $\mathbf{y}(t) = C\mathbf{x}(t)$ and $Q = C^T C$.

As shown in Chapter 3, $J(K^*, \theta_{AB}^*)$ (the saddle point of interest) is optimum if and only if

$$J(K^*, \theta_{AB}^*) \leq J(K^*, \theta_{AB}^*) \leq J(K, \theta_{AB}^*). \quad (4.2)$$

Following, we show that the solution may not be unique, however, if there are multiple solutions, all optimal LQR costs must be equal. If it is the case that more than one solution exists, then it does not matter which solution is chosen in the final design.

Theorem 4.1 (Uniqueness of Solution): *If there are more than one (K, θ) which satisfy (4.2) then their associated LQR costs must be equal and any one of the solutions can be used to compute the minimax control.*

Proof: (This proof follows from [36]). Assume there exist (K_1, θ_1) and (K_2, θ_2) such that

$$J(K_1, \theta) \leq J(K_1, \theta_1) \leq J(K, \theta_1) \quad \forall K, \theta \quad (4.3)$$

and

$$J(K_2, \theta) \leq J(K_2, \theta_2) \leq J(K, \theta_2) \quad \forall K, \theta. \quad (4.4)$$

Setting $\theta = \theta_2$ and $K = K_2$ in (4.3), we get

$$J(K_1, \theta_2) \leq J(K_1, \theta_1) \leq J(K_2, \theta_1).$$

From (4.4)

$$J(K_2, \theta_1) \leq J(K_2, \theta_2) \Rightarrow J(K_1, \theta_1) \leq J(K_2, \theta_2) \quad (4.5)$$

Similarly, setting $\theta = \theta_1$ and $K = K_1$ in (4.4), we get

$$J(K_2, \theta_1) \leq J(K_2, \theta_2) \leq J(K_1, \theta_2).$$

From (4.3)

$$J(K_1, \theta_2) \leq J(K_1, \theta_1) \Rightarrow J(K_2, \theta_2) \leq J(K_1, \theta_1). \quad (4.6)$$

Equations (4.5) and (4.6) imply $J(K_1, \theta_1) = J(K_2, \theta_2)$. It follows that if there are k solutions $J(K_k, \theta_k)$ that satisfy (4.2) then $J(K_i, \theta_i) = J(K_j, \theta_j)$ for any $i, j = 1, 2, \dots, k$. Thus, any one of the solutions (K_i, θ_i) for $i = 1, 2, \dots, k$ may be used for the final control design. \square

Assuming a saddle point exists, it is necessarily true that

$$\theta_{AB}^* = \arg \max_{\theta_{AB} \in \Omega} \int_0^{\infty} \mathbf{x}^T(t) (K^{*T} R K^* + C^T C) \mathbf{x}(t) dt. \quad (4.7)$$

This fact is used in the following section. From this viewpoint we seek a two-step iterative algorithm, that first solves the LQR minimization for K , and second solves (4.7) for θ_{AB} , such that the algorithm converges to (K^*, θ_{AB}^*) .

Some Useful Results from LQR Control Theory

Since we are seeking a controller in the form of standard LQR state-feedback it can be shown that the minimization of (4.1) over $K \in \mathcal{K}$ yields the following sets of identities.

First Set:

$$K^T R K + C^T C = -[(A - BK)^T P + P(A - BK)] \quad (4.8)$$

for any set $\theta_{AB} \in \Omega$ where P , symmetric and positive definite, is the solution to the standard Riccati equation of (3.11) and the feedback gain K is given by (3.10). We also know from LQR theory that for a given $[A, B]$, the optimal cost is given by

$$\min_{K \in \mathcal{K}} J(K, \theta_{AB}) = \mathbf{x}(0)^T P \mathbf{x}(0). \quad (4.9)$$

Second Set:

Using the identity $\mathbf{z}^T \Phi \mathbf{z} \triangleq \text{tr}\{\Phi \mathbf{z} \mathbf{z}^T\}$, where $\text{tr} \equiv \text{trace}$, the standard linear operator, the cost function from (4.1) can be written as

$$J(K, \theta_{AB}) = \text{tr} \left[\int_0^\infty Z(K) \mathbf{x}(t) \mathbf{x}^T(t) \right] dt, \quad (4.10)$$

where $Z(K)$ is given by

$$Z(K) \triangleq K^T R K + C^T C,$$

and $\mathbf{x}(t)$ is a function of θ_{AB} . Using the fact that $Z(K)$ is independent of time, (4.10) becomes

$$J(K, \theta_{AB}) = \text{tr} \left[Z(K) \int_0^\infty \mathbf{x}(t) \mathbf{x}^T(t) dt \right]. \quad (4.11)$$

Since the closed-loop system must be stable for the cost to be finite, there exists a positive definite matrix L which solves the associated Lyapunov equation,

$$(A - BK)L + L(A - BK)^T + \mathbf{x}_0 \mathbf{x}_0^T = \mathbf{0} \quad (4.12)$$

where $\mathbf{x}_0 \triangleq \mathbf{x}(0)$. The solution L of (4.12) is actually a function of θ_{AB} and is given by

$$L = \int_0^\infty \mathbf{x}(t) \mathbf{x}^T(t) dt. \quad (4.13)$$

Equation (4.13) is sometimes referred to as the controllability grammian. Thus, (4.11) becomes

$$J(K, \theta_{AB}) = \text{tr} [Z(K)L]. \quad (4.14)$$

These sets of identities lead to two possible iterative approaches for finding $[K^*, \theta_{AB}^*]$ and are given in the following sections.

Iterative Solution Approaches

The first approach follows from the first set of identities using equations (4.8)-(4.9).

Algorithm 1:

Let $[A_{(j)}, B_{(j)}]$ be given at the j^{th} iterate.

- I. (minimize) Solve the Riccati equation of (4.15) and the feedback control law of (4.16) for $P_{(j)}$ and $K_{(j)}$, respectively.

$$A_{(j)}^T P_{(j)} + P_{(j)} A_{(j)} - P_{(j)}^T B_{(j)} R^{-1} B_{(j)}^T P_{(j)} + C^T C = 0. \quad (4.15)$$

$$K_{(j)} = R^{-1} B_{(j)}^T P_{(j)}. \quad (4.16)$$

- II. (maximize) Solve (4.17) for $[A_{(j+1)}, B_{(j+1)}]$.

$$[A_{(j+1)}, B_{(j+1)}] = \arg \max_{\theta_{AB} \in \Omega} \mathbf{x}_0^T P \mathbf{x}_0 \quad (4.17)$$

subject to

$$(A - BK_{(j)})^T P + P(A - BK_{(j)}) + K_{(j)}^T R K_{(j)} + C^T C = 0.$$

where $P = P(A, B)$ in (4.17) because of the above constraint.

- III. (check convergence) If $\| [A_{(j+1)}, B_{(j+1)}] - [A_{(j)}, B_{(j)}] \|$ is less than some desired tolerance, then stop. Otherwise, let $[A_{(j+1)}, B_{(j+1)}] \rightarrow [A_{(j)}, B_{(j)}]$ and continue at step I.

The algorithm may be initiated by selecting the nominal parameter values of Ω for $[A_{(0)}, B_{(0)}]$.

The second approach follows from the second set of identities using equations (4.12)-(4.14) and also equations (3.10) and (3.11).

Algorithm 2:

Let $[A_{(j)}, B_{(j)}]$ be given at the j^{th} iterate.

- I. (minimize) Solve the Riccati equation of (4.18) and the feedback control law of (4.19) for $P_{(j)}$ and $K_{(j)}$, respectively.

$$A_{(j)}^T P_{(j)} + P_{(j)} A_{(j)} - P_{(j)}^T B_{(j)} R^{-1} B_{(j)}^T P_{(j)} + C^T C = 0. \quad (4.18)$$

$$K_{(j)} = R^{-1} B_{(j)}^T P_{(j)}. \quad (4.19)$$

- II. (maximize) Solve (4.20) for $[A_{(j+1)}, B_{(j+1)}]$.

$$[A_{(j+1)}, B_{(j+1)}] = \arg \max_{\theta_{AB} \in \Omega} -tr [Z(K_{(j)})L] \quad (4.20)$$

subject to

$$(A - BK_{(j)})L + L(A - BK_{(j)})^T + \mathbf{x}_0 \mathbf{x}_0^T = \mathbf{0}.$$

where $L = L(A, B, \mathbf{x}_0)$ in (4.20) because of the above constraint.

- III. (check convergence) If $\|[A_{(j+1)}, B_{(j+1)}] - [A_{(j)}, B_{(j)}]\|$ is less than some desired tolerance, then stop. Otherwise, let $[A_{(j+1)}, B_{(j+1)}] \rightarrow [A_{(j)}, B_{(j)}]$ and continue at step I.

Remarks:

- In step III of both iterative approaches, the norm on the differences would actually be performed using the equivalent vector of parameters $\theta_{AB}^{(j+1)}$ and $\theta_{AB}^{(j)}$.
- The first iterative approach is dependent on the initial conditions through the final optimal cost equation of (4.9); the second iterative approach is dependent on the initial conditions through the controllability grammian of (4.12). However, this dependence on \mathbf{x}_0 can be removed if we start with the assumption

that \mathbf{x}_0 is a random vector with known mean \bar{m} and covariance V and the objective in (4.1) is an expectation over \mathbf{x}_0 . In that case, $\dot{\mathbf{x}}_0 \mathbf{x}_0^T$ may be replaced by $V + \bar{m} \bar{m}^T$. Another alternative is to use the worst initial condition of unit magnitude as in [69].

- Equivalence of each iterative approach is implied by virtue of existence of the LQR minimization solution and thus the existence of the associated controllability grammian of (4.12).
- The maximization in step II of **Algorithm 1** may be stated more precisely.

Let the symmetric matrix P be defined as

$$P \triangleq \begin{bmatrix} p_1 & p_2 & p_3 & \cdots & p_{n_a-1} & p_{n_a} \\ p_2 & p_{n_a+1} & p_{n_a+2} & \cdots & p_{2n_a-2} & p_{2n_a-1} \\ p_3 & p_{n_a+2} & p_{2n_a} & p_{2n_a+1} & \cdots & \vdots \\ \vdots & \vdots & \vdots & \vdots & \ddots & \vdots \\ p_{n_a-1} & p_{2n_a-2} & \cdots & \cdots & \cdots & \vdots \\ p_{n_a} & p_{2n_a-1} & \cdots & \cdots & \cdots & p_{\frac{n_a(n_a+1)}{2}} \end{bmatrix}$$

Next, let $f(\xi) \triangleq \mathbf{x}_0^T P \mathbf{x}_0$ where ξ is given as

$$\xi \triangleq \left[a_1 \ a_2 \ \cdots \ a_{n_a} \ b_1 \ b_2 \ \cdots \ b_{n_b} \ p_1 \ p_2 \ \cdots \ p_{\frac{n_a(n_a+1)}{2}} \right]^T.$$

Solve (4.21) for $\xi_{(k+1)}$.

$$\xi_{(k+1)} = \arg \max_{\xi \in \mathbb{R}^N} f(\xi) \quad (4.21)$$

subject to

$$\theta_{AB} \in \Omega \quad (4.22)$$

and

$$(A - BK_{(j)})^T P + P(A - BK_{(j)}) + K_{(j)}^T R K_{(j)} + C^T C = \mathbf{0}, \quad (4.23)$$

where $N \triangleq n_a + n_b + \frac{n_a(n_a+1)}{2}$.

- Similarly, the maximization in step II of Algorithm 2 may be stated more precisely.

Let the symmetric matrix L be defined as

$$L \triangleq \begin{bmatrix} l_1 & l_2 & l_3 & \cdots & l_{n_a-1} & l_{n_a} \\ l_2 & l_{n_a+1} & l_{n_a+2} & \cdots & l_{2n_a-2} & l_{2n_a-1} \\ l_3 & l_{n_a+2} & l_{2n_a} & l_{2n_a+1} & \cdots & \vdots \\ \vdots & \vdots & \vdots & \vdots & \ddots & \vdots \\ l_{n_a-1} & l_{2n_a-2} & \cdots & \cdots & \cdots & \vdots \\ l_{n_a} & l_{2n_a-1} & \cdots & \cdots & \cdots & \frac{l_{n_a(n_a+1)}}{2} \end{bmatrix}$$

Next, let $f(\xi) \triangleq \text{tr} [Z(K_{(j)})L]$ where ξ is given as

$$\xi \triangleq \left[a_1 \ a_2 \ \cdots \ a_{n_a} \ b_1 \ b_2 \ \cdots \ b_{n_b} \ l_1 \ l_2 \ \cdots \ l_{\frac{n_a(n_a+1)}{2}} \right]^T.$$

Solve (4.24) for $\xi_{(k+1)}$.

$$\xi_{(k+1)} = \arg \max_{\xi \in \mathbb{R}^n} f(\xi) \quad (4.24)$$

subject to

$$\theta_{AB} \in \Omega$$

and

$$(A - BK_{(j)})L + L(A - BK_{(j)})^T + \mathbf{x}_0 \mathbf{x}_0^T = \mathbf{0}.$$

where $\aleph \triangleq n_a + n_b + \frac{n_a(n_a+1)}{2}$.

- The primary difference between the algorithms is that the first algorithm results from a parameterization in the elements of the Riccati matrix P and the second results from a parameterization in the elements of the grammian matrix L .
- With these simple changes in notation we still check for convergence using $\theta_{AB}^{(j+1)}$ and $\theta_{AB}^{(j)}$.

Although it is true that multiple saddle points exhibit equivalent LQR costs, it is possible for the algorithm to converge to a local saddle-point and not necessarily

a global saddle-point. For this reason, it is necessary to apply K^* to all plants within the plant set Ω to insure that (K^*, θ_{AB}^*) is a global maximum or stated another way, to insure that the control gain K^* does not cause destabilization for any other plants. It is not practical to test the optimal controller on all plants; therefore, a selection of plants from the plant set Ω must be chosen to determine the likelihood that all plants in Ω are stabilized by K^* . One approach is to select N_e sub-ellipsoids of the bounding ellipsoid Ω such that $\theta_0 = \Omega_1 \subset \Omega_2 \subset \dots \subset \Omega_{N_e} \subset \Omega$. Note that the limiting case Ω_1 is actually the center of the ellipsoid Ω and is simply given by the nominal parameters θ_0 . For each sub-ellipsoid, Ω_i , select N_b plants, θ_{AB}^{ij} , $j = 1, 2, \dots, N_b$, on the boundary, apply the optimal gain K^* , and compute the LQR cost $J(K^*, \theta_{AB}^{ij})$. This procedure checks a total of $N_e N_b$ plants within Ω . If (K^*, θ_{AB}^*) is a global maximum then according to (4.2) the following must hold

$$J(K^*, \theta_{AB}^{ij}) \leq J(K^*, \theta_{AB}^*).$$

Examples

In all examples, unless otherwise stated, the convergence criterion is given by

$$\|\theta_{AB}^{(j+1)} - \theta_{AB}^{(j)}\|_2 \leq tol$$

where the tolerance is $tol = 0.0001$.

Example 1: Two System Parameters (Stabilizable) The first example is for a first-order system with two uncertain parameters, a_1 and b_1 . The output matrix $C = 1$, the LQR weight $R = r_1$, and the initial condition $x(0) = x_0$. The positive symmetric matrix Γ of (3.32) has three parameters, γ_1, γ_2 and γ_3 while the nominal vector θ_0 of (3.31) has two parameters θ_{01} and θ_{02} . The Riccati matrix of

(4.15) is a scalar, i.e., $P = p_1$ and the feedback gain of (4.16) is scalar, i.e., $K = k_1$. The number of parameters to maximize over is $N = 3$, thus, ξ of (4.21) is given by $\xi = [a_1 \ b_1 \ p_1]^T \triangleq [\xi_1 \ \xi_2 \ \xi_3]^T$. The function of (4.21) reduces to

$$f(\xi) = \xi_3 x_0^2.$$

The inequality constraint given by (4.22) is given by

$$[(\xi_1 - \theta_{01}), (\xi_2 - \theta_{02})]^T \Gamma [(\xi_1 - \theta_{01}), (\xi_2 - \theta_{02})] - 1 \leq 0 \quad (4.25)$$

and the equality constraint given by (4.23) is simplified to

$$-2(\xi_1 + \xi_2 k_1) \xi_3 + r_1 k_1^2 + 1 = 0. \quad (4.26)$$

While the existence of a solution has not been shown, it is worthwhile to consider where the solution may reside. If the domain of ξ is convex, then the function $f(\xi)$, which is convex by linearity, will have its solution at an extreme point of the domain [73, Theorem 3, page 119]. Consider the following definition of convexity.

Definition 4.1 *A set Ω_c in \mathbb{R}^n is said to be convex if for every $\xi_a, \xi_b \in \Omega_c$ and every real number α , $0 < \alpha < 1$, the point $\alpha \xi_a + (1 - \alpha) \xi_b \in \Omega_c$.*

Let the domain defined by the equality constraint (4.26) be represented by Ω_ξ . The domain of ξ is $\Omega_N \triangleq \Omega \cap \Omega_\xi$ where Ω is the ellipsoidal domain given by the inequality constraint (4.25) and is defined in (3.30). It is well known that the intersection of any collection of convex sets is also convex [73, see Appendix B]. In order for Ω_N to be convex it is sufficient to show Ω_ξ to be convex. While it would be helpful for Ω_N to be convex, this is, in general, not true. It can be seen by further analysis of (4.26) that Ω_ξ is, in general, not convex and thus Ω_N is, in general, not convex. We show this through theorem and proof.

Theorem 4.2 *In general, Ω_ξ , defined by (4.26), is not convex and therefore, $\Omega_N \triangleq \Omega \cap \Omega_\xi$, where Ω is defined by (4.25), is, in general, not convex.*

Proof: {Proof by counterexample} Assume there exist two vectors ξ_a and $\xi_b \in \Omega_\xi$ such that $\alpha\xi_a + (1 - \alpha)\xi_b \in \Omega_\xi$ for any scalar α where $0 < \alpha < 1$. From (4.26), this is equivalent to saying

$$h(\alpha\xi_a + (1 - \alpha)\xi_b) = d \text{ for any } \alpha : 0 < \alpha < 1 \quad (4.27)$$

where $h(\xi) \triangleq (\xi_1 + \xi_2 k_1)\xi_3$ and $d \triangleq \frac{r_1 k_1^2 + 1}{2}$. Defining $\xi_a \triangleq [\xi_{a1} \ \xi_{a2} \ \xi_{a3}]^T$ and $\xi_b \triangleq [\xi_{b1} \ \xi_{b2} \ \xi_{b3}]^T$ and using the fact that $h(\xi) = d, \forall \xi \in \Omega_\xi$, it can be shown, with some algebraic manipulation, that (4.27) reduces to

$$h(\alpha\xi_a + (1 - \alpha)\xi_b) = \left(\alpha(1 - \alpha) \left(\frac{\xi_{a3}^2 + \xi_{b3}^2}{\xi_{a3}\xi_{b3}} \right) + (1 - 2\alpha) \right) d$$

for any α such that $0 < \alpha < 1$. Hence, using (4.27) again, we obtain

$$\begin{aligned} \alpha &= 1 - \left(\frac{\xi_{a3}^2 + \xi_{b3}^2}{2\xi_{a3}\xi_{b3}} \right)^{-1} \\ &= 1 - \left(\frac{(\xi_{a1} + \xi_{a2}k_1)^2 + (\xi_{b1} + \xi_{b2}k_1)^2}{2(\xi_{a1} + \xi_{a2}k_1)(\xi_{b1} + \xi_{b2}k_1)} \right)^{-1} \end{aligned} \quad (4.28)$$

Note that (4.28) is independent of r_1 . Equation (4.28) is generally not true for any arbitrary selection of $\xi_a, \xi_b \in \Omega_\xi$ and for any $\alpha \in (0, 1)$, as can be seen by the following example.

Let $\Gamma = I_2 \times 2$, the weight $r_1 = 1$, the nominal values $[\theta_{01}, \theta_{02}] = [2, 0.2]^T$, and the initial condition $x_0 = 1$. Further, let $[\xi_{a1}, \xi_{a2}] = [1 \ 1]$ and $[\xi_{b1}, \xi_{b2}] = [3 \ 1]$ (although each point satisfies the inequality constraint (4.25), this is not a requirement since the intersection of Ω and Ω_ξ has not yet been taken). We see that (4.28) is only true for $\alpha = \frac{1}{5}$ and not for any arbitrary $\alpha \in (0, 1)$. Therefore, in general, Ω_ξ as defined in (4.26) is not convex. It follows that, in general, the intersection of the

convex domain Ω with the non-convex domain Ω_ξ is also non-convex. \square

Remark: This observation does not preclude the possibility that a saddle point exists on the boundary of Ω .

Indeed, for this example, i.e., $\Gamma = I_2 \times 2$, the weight $r_1 = 1$, the nominal values $[\theta_{01}, \theta_{02}] = [2, 0.2]^T$, and the initial condition $x_0 = 1$, the system exhibits a saddle point on the boundary of Ω . The saddle point is shown in Figure 19. **Algorithm 1** converged in 15 iterations to the *worst-case* plant parameters $\theta_{AB}^* = [1.0002, 0.1337]^T$. The optimal gain associated with these parameters is $K^* = 0.0664$ and the LQR cost is $J^* = 0.4967$.

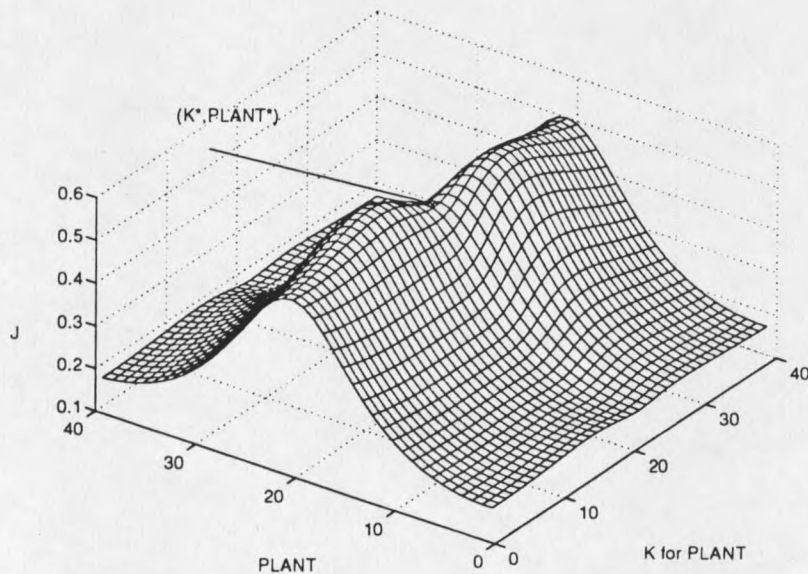


Figure 19. Illustration of saddle point on the boundary of Ω for Example 1.

In Figure 20, "PLANT" is equivalent to θ_{AB} of (4.2). The horizontal axis represents 40 plants uniformly distributed along the boundary of Ω . The vertical axis is the LQR cost for a controller/plant pair. The optimal cost, $J(K^*, \theta_{AB}^*)$, is shown as a horizontal dashed line. The curve above the optimal cost line is for the optimal

plant θ_{AB}^* but with the application of the LQR gains for the plants distributed around the perimeter of Ω . The curve below the optimal cost line is for the plants distributed around the perimeter of Ω and with the optimal control gain K^* applied. Clearly, Figure 20 reveals that the saddle point condition of (4.2) is at least satisfied for those plants around the perimeter of Ω .

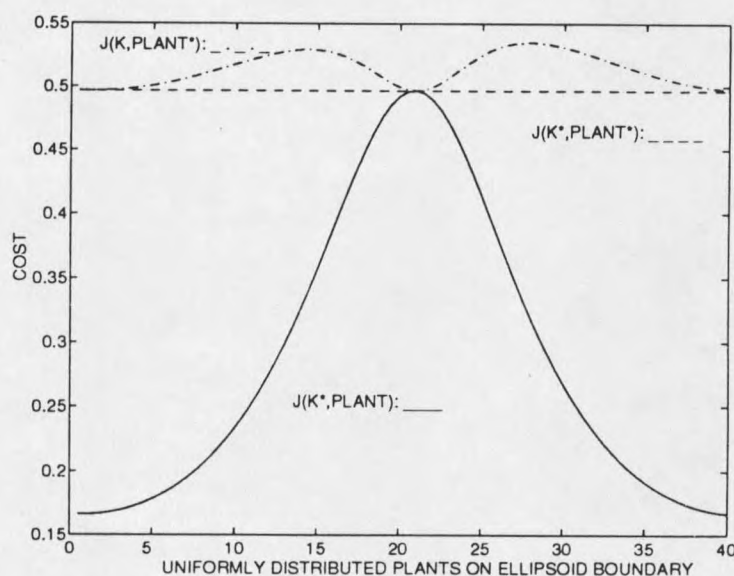


Figure 20. Illustration in two dimension of saddle point condition for Example 1.

Remark: The controllability matrix, $\mathcal{C} = b_1$, is singular for some plants in the ellipsoid, Ω . Although the system is not controllable it is at least stabilizable. If $\theta_0 = [0, 0.2]^T$, the system is not controllable nor is it stabilizable for some of the plants in the ellipsoid. For this system **Algorithm 1** fails to converge. It is well known that the solution to the standard Riccati equation exists as long as the system is at least stabilizable and detectable. Since **Algorithm 1** solves a Riccati equation, it is *necessary* for all plants in Ω to be at least stabilizable. To support this observation consider the following example. We obtain the same results using **Algorithm 2**.

Example 2: Two System Parameters (Controllable, Unstable) The

following example is an uncertain system where all plants in the region Ω are controllable, yet are possibly unstable. The description of the uncertain system is summarized below.

- $\Gamma = I_2 \times 2$
- $r_1 = 1$
- $\theta_0 = [0.1 \ 2]^T$
- $x_0 = 1$

After 14 iterations Algorithm 1 converged to the following optimal values:

- $\theta_{AB}^* = [0.4627 \ 1.1733]^T$
- $K^* = 1.4692$
- $J(K^*, \theta_{AB}^*) = 1.2522$

These results are shown graphically in Figure 21. Note that the cost increases sharply as other optimal LQR control gains are applied to the plants that are near to the plant given by θ_{AB}^* . This is really of no concern, however, the question remains as to whether the gain given by K^* results in larger costs than $J(K^*, \theta_{AB}^*)$ when applied to plants in the interior of Ω .

Figure 22 shows the LQR cost for plants located around the perimeter of ellipsoids contained in Ω . The size of the interior ellipsoids are monotonically decreasing in size. The limiting case is the single point corresponding to the center of the ellipsoid. The limiting point becomes a horizontal line at an LQR cost of 0.5198. As is evident, the true saddle point is located on the boundary of Ω . For several other examples

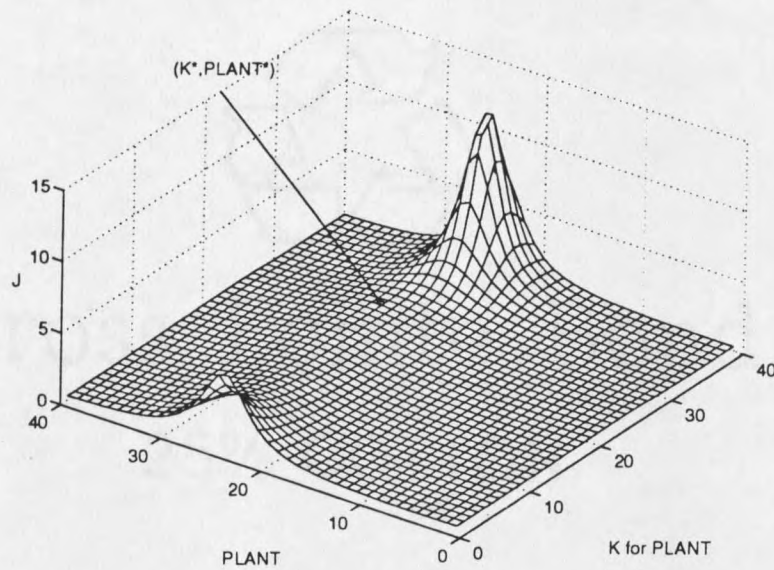


Figure 21. Illustration of saddle point on the boundary of Ω for Example 2.

we noted that all the solutions tended to the boundary of the ellipsoid. A proof for existence of solution is not provided for the continuous time problem.

Discrete-Time System Problem Statement

The system is described by (3.35) and (3.36). As discussed in Chapter 3, the form of the control that is of interest here is linear state feedback

$$u(k) = -Kx(k).$$

where $K = K_\infty$ of (3.20). The set of stabilizing controllers is defined by

$$\mathcal{K} \triangleq \{K : K \text{ stabilizes } G(z) \forall \theta_{FH} \in \Omega\}.$$

Those cases where \mathcal{K} is nonempty are of interest.

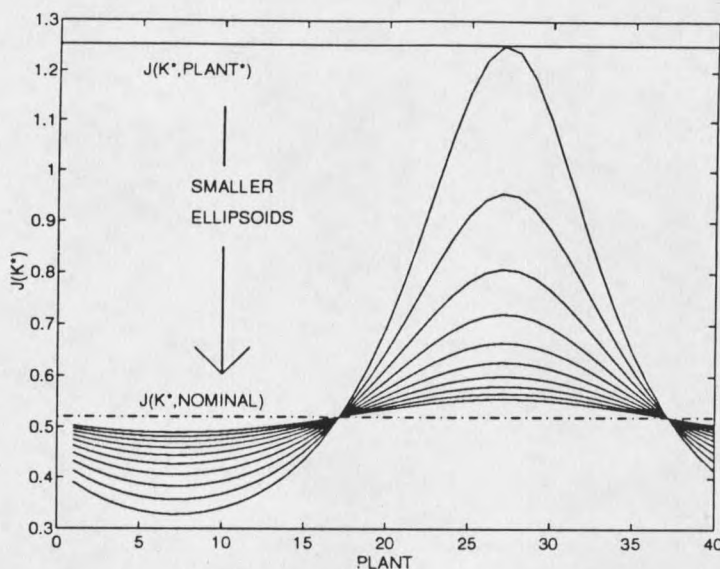


Figure 22. LQR costs for plants within interior of uncertainty region using $K^* = 1.4692$; Example 2.

Statement of Problem: Find a controller $K^* \in \mathcal{K}$ that stabilizes $G(z) \forall \theta_{FH} \in \Omega$ and is optimum in the sense of the minimaximization of the quadratic cost function

$$J(K, \theta_{FH}) = \sum_{k=0}^{N \rightarrow \infty} [\mathbf{x}(k)^T (K^T R K + C^T C) \mathbf{x}(k)] \quad (4.29)$$

where R is symmetric and positive definite. Since the system is SISO, $R \in \mathbb{R}$ is scalar and must be greater than 0. This problem is equivalent to finding a saddle point solution. Note that (4.29) is equivalent to (3.14) under the condition that $\mathbf{y}(k) = C\mathbf{x}(k)$ and $Q = C^T C$.

As shown in Chapter 3, $J(K^*, \theta_{FH}^*)$ (the saddle point of interest) is optimum if and only if

$$J(K^*, \theta_{FH}) \leq J(K^*, \theta_{FH}^*) \leq J(K, \theta_{FH}^*). \quad (4.30)$$

As in the case for the continuous time system **Theorem 4.1** holds for the discrete case. Assuming a saddle point exists, it is necessarily true that

$$\theta_{FH}^* = \arg \max_{\theta_{FH} \in \Omega} \sum_{k=0}^{N \rightarrow \infty} [\mathbf{x}(k)^T (K^T R K + C^T C) \mathbf{x}(k)]. \quad (4.31)$$

This fact is used in the following section. From this viewpoint we seek a two-step iterative algorithm, that first solves the LQR minimization for K , and second solves (4.31) for θ_{FH} , such that the algorithm converges to (K^*, θ_{FH}^*) .

Iterative Solution Approach

The iterative approach that follows is similar to **Algorithm 1** of the continuous-time problem. In this algorithm we make use of (3.18), the infinite-horizon discrete-time Riccati equation. We also make use of the discrete-time Lyapunov equation

$$(F - HK)^T P (F - HK) - P + K^T R K + C^T C = 0. \quad (4.32)$$

For a stable matrix $F - HK$, there exists a positive definite matrix P which satisfies (4.32) [46].

Algorithm 3:

Let $[F_{(j)}, H_{(j)}]$ be given at the j^{th} iterate.

- I. (minimize) Solve the Riccati equation of (4.33) and the feedback control law of (4.34) for $P_{(j)}$ and $K_{(j)}$, respectively.

$$P_{(j)} = F^T P_{(j)} F - F^T P_{(j)} H [R + H^T P_{(j)} H]^{-1} H^T P_{(j)} F + C^T C \quad (4.33)$$

$$K_{(j)} = [R + H^T P_{(j)} H]^{-1} H^T P_{(j)} F. \quad (4.34)$$

- II. (maximize) Solve (4.35) for $[F_{(j+1)}, H_{(j+1)}]$.

$$[F_{(j+1)}, H_{(j+1)}] = \arg \max_{\theta_{FH} \in \Omega} \mathbf{x}_0^T P \mathbf{x}_0 \quad (4.35)$$

subject to

$$(F - HK_{(j)})^T P (F - HK_{(j)}) - P + K_{(j)}^T R K_{(j)} + C^T C = 0.$$

- III. (check convergence) If $\| [F_{(j+1)}, H_{(j+1)}] - [F_{(j)}, H_{(j)}] \|$ is less than some desired tolerance, then stop. Otherwise, let $[F_{(j+1)}, H_{(j+1)}] \rightarrow [F_{(j)}, H_{(j)}]$ and continue at step I.

The algorithm may be initiated by selecting the nominal parameter values of Ω for $[F_{(0)}, H_{(0)}]$.

On The Nature Of The Solution Of Algorithm 3

From the previous sections dealing with the continuous time problem we saw that the examples provided had solutions on the boundary of the ellipsoid. Here we look at **Algorithm 3** for the discrete problem.

Consider the first-order problem where there is only uncertainty in the parameter of F and the parameter of H is constant. The uncertain parameter is simply a symmetric interval about some nominal value a_0 . The state-space equations are given by

$$x(k+1) = ax(k) + bu(k) \quad (4.36)$$

and

$$y(k) = x(k).$$

First consider the minimization portion of **Algorithm 3**. The Riccati equation of (4.33) for the solution to the control law is given by

$$p = a^2 p - \frac{a^2 b^2 p^2}{r + b^2 p} + 1,$$

which simplifies to a quadratic polynomial in p

$$b^2 p^2 + ((1 - a^2)r - b^2)p - r = 0.$$

Using the positive solution to this polynomial for any value of a in the corresponding uncertainty region, we know from (4.34) that

$$K = \frac{abp}{r + b^2p}.$$

Thus K is a scalar which may be positive or negative depending on the the values of a and b . Next, consider the maximization portion of Algorithm 3. Equation (4.35) reduces to

$$a = \arg \max_{a,p} px_0^2 \quad (4.37)$$

subject to

$$(a - a_0)^2 \gamma \leq 1$$

and

$$((a - bK)^2 - 1)p + rK^2 + 1 = 0. \quad (4.38)$$

Solving (4.38) for p we arrive at

$$p = \frac{1 + rK^2}{1 - (a - bK)^2}.$$

If we assume that K stabilizes (4.36) for all values of a , we see that $|(a - bK)|$ is always less than 1. Since $r > 0$ we note that $p > 0$ and is finite. Next, if we substitute p above into (4.37) we obtain

$$a = \arg \max_a \frac{(1 + rK^2)x_0^2}{1 - (a - bK)^2}$$

which is equivalent to

$$a = \arg \max_a (a - bK)^2.$$

The function being maximized is a quadratic function. Furthermore, since we have assumed that K stabilizes (4.36) over all a then we know that $|(a - bK)| < 1$ which implies $(a - bK)^2$ is a convex function. Hence, the solution resides on the boundary [73, Theorem 3, page 119].

As expected, the existence of the solution to the maximization problem relies on the condition that K stabilizes (4.36) for all values of a . A sufficient condition for the existence of the maximization problem is shown in **Theorem 4.3**.

Theorem 4.3 (Existence of Maximization in Algorithm 3): *If the gain K given in (4.34) stabilizes all plants $\theta_{FH} \in \Omega$ and furthermore, for all plants $\theta_{FH} \in \Omega$ it is true that $\sigma_M(F - HK) < 1$ (σ_M denotes maximum singular value) then*

$$\max_{\theta_{FH} \in \Omega} \mathbf{x}_0^T P \mathbf{x}_0$$

subject to

$$(F - HK)^T P (F - HK) - P + K^T R K + C^T C = 0$$

exists.

Before proving this theorem, we shall make use of the following lemmas.

Lemma 4.1 *For any $n \times n$ matrices P and Y such that $P > 0$, $Y \geq 0$, the following inequalities are satisfied:*

$$\lambda_m(Y) \text{tr}(P) \leq \text{tr}(PY) \leq \lambda_M(Y) \text{tr}(P)$$

where λ_m and λ_M denote the minimum and maximum eigenvalues, respectively.

Lemma 4.1 was taken from [74] and the proof can be found in [75].

Lemma 4.2 *For the discrete Lyapunov equation $X^T P X - P + Z = 0$ and $Z \geq 0$, the following inequality is true*

$$\frac{\text{tr}(Z)}{1 - \lambda_m(X X^T)} \leq \text{tr}(P) \leq \frac{\text{tr}(Z)}{1 - \lambda_M(X X^T)}$$

The proof of **Lemma 4.2** is given in [76].

Proof: (Theorem 4.3) Making use of the fact $\mathbf{x}_0^T P \mathbf{x}_0 = \text{tr}(P \mathbf{x}_0 \mathbf{x}_0^T)$ and Lemma 4.1 where $Y \triangleq \mathbf{x}_0 \mathbf{x}_0^T$, we see that

$$\max_{\theta_{FH} \in \Omega} \mathbf{x}_0^T P \mathbf{x}_0$$

subject to

$$(F - HK)^T P (F - HK) - P + K^T R K + C^T C = 0$$

is less than or equal to

$$\max_{\theta_{FH} \in \Omega} \text{tr}(P) \lambda_M(Y)$$

subject to

$$(F - HK)^T P (F - HK) - P + K^T R K + C^T C = 0.$$

Using the results of Lemma 4.2 and letting $X \triangleq F - HK$ and $Z \triangleq K^T R K + C^T C$ we obtain the following.

$$\lambda_M(Y) \max_{\theta_{FH} \in \Omega} \text{tr}(P)$$

subject to

$$X^T P X - P + Z = 0$$

is less than or equal to

$$\lambda_M(Y) \max_{\theta_{FH} \in \Omega} \frac{\text{tr}(Z)}{1 - \lambda_M(X X^T)}.$$

Since $\sigma_m(X) \leq \min_i |\lambda_i(X)| \leq \max_i |\lambda_i(X)| \leq \sigma_M(X)$ for $i = 1, 2, \dots, n$ [77], where the definition of singular value is given by $\sigma \triangleq \sqrt{\lambda(X X^T)}$, we see that

$$\max_{\theta_{FH} \in \Omega} \frac{\text{tr}(Z)}{1 - \lambda_M(X X^T)} \equiv \max_{\theta_{FH} \in \Omega} \frac{\text{tr}(Z)}{1 - \sigma_M^2(X)}.$$

Thus, if $\sigma_M(F - HK) < 1 \quad \forall \theta_{FH} \in \Omega$ then the original maximization problem has a bounded solution. Hence, a sufficient condition for the existence of solution to the maximization problem of Algorithm 3 has been shown. \square

To show for a given K that it stabilizes all plants $\theta_{FH} \in \Omega$ is not a trivial matter and is left for future research. **Theorem 4.3** does not tell us where the solution resides and this is a subject of continuing research.

Set-membership Control Problem

Following is an example of set-membership identification and control problem. The ellipsoid bounding algorithm of [62] is used for set-membership identification. The example is in discrete-time; therefore, we use **Algorithm 3** for the robust control design. The states of the system are estimated using a Kalman filter. Implementation of a set-membership control problem raises an interesting question when one is employing a Kalman filter for state estimation; which plant within the uncertainty region does one select for use in the Kalman filter? For this example we take the parameters of the center of the ellipsoid for use in the Kalman filter. The reasoning behind this selection is that the center of the ellipsoid is "likely" closer to the actual plant than the worst-case plant associated with the robust control design and will likely offer a better estimate of the true system states.

Second Order Servo Example Consider the controlled plant (this example is found in [78, page 385])

$$\mathbf{x}(k+1) = \begin{bmatrix} 1.5 & 1 \\ -0.5 & 0 \end{bmatrix} \mathbf{x}(k) + \begin{bmatrix} 1 \\ 0.6 \end{bmatrix} [u(k) + w(k)]$$

$$y(k) = [1 \ 0] \mathbf{x}(k) + v(k)$$

where $w(k)$ and $v(k)$ are independent Gaussian noise disturbances. The object of this servo control is to determine an optimum controller

$$u(k) = -K^T \mathbf{x}(k) + Vr(k)$$

minimizing the cost function

$$J = \sum_{k=1}^{\infty} [\Psi^T(k)Q\Psi(k) + R(u(k) - u_{ss})^2]$$

where

$$\Psi^T(k) = [x_1(k) \ x_2(k) \ r(k)],$$

$$Q = \begin{bmatrix} 1 & 0 & -1 \\ 0 & 0 & 0 \\ -1 & 0 & 1 \end{bmatrix},$$

$$u_{ss} = u(\infty),$$

and

$$R = 1.$$

The command variable $r(k)$ may take the values $(-1, 0, 1)$. The sampling period $T = 1$. The variable V is a scaling factor determined from the condition of zero steady-state control error. The scaling factor is adjusted depending on the gain vector K used for state feedback control. We note that this servo example is unusual in the way we are using the variable V for adjusting the steady-state error. A more popular method is to remove the gain block V and introduce an integrator into the forward path of the system (see, e.g., [46, page 850]). In order to keep the example simple and to follow the example as given in [78, page 385], we did not introduce the integrator.

The states are estimated using a Kalman filter. The associated equations are given below and can be found in numerous sources, see for example [46, 78]. We use F_0 and H_0 to denote the nominal plant given by the center of the bounding ellipsoid. Using steps (a) and (b) below $\hat{x}(k+1|k+1)$ can be solved given the Kalman gain $K_e(k+1)$ and the initial estimate $\hat{x}(k|k)$.

$$(a) \ \hat{x}(k+1|k) = F_0\hat{x}(k|k) + H_0u(k),$$

$$(b) \hat{x}(k+1|k+1) = \hat{x}(k+1|k) + K_e(k+1)[y(k+1) - C\hat{x}(k+1|k)].$$

For an initial Riccati matrix $P_e(k|k)$ the Kalman gain $K_e(k+1)$ is solved using steps (c) and (d) below. The Riccati matrix P_e is updated in step (e).

$$(c) P_e(k+1|k) = F_0 P_e(k|k) F_0^T + H_0 Q_e H_0^T,$$

$$(d) K_e(k+1) = P_e(k+1|k) C^T [C P_e(k+1|k) C^T + R_e]^{-1},$$

$$(e) P_e(k+1|k+1) = [I - K_e(k+1)C] P_e(k+1|k).$$

The adjustable weights which are the dual to the weights seen in the linear quadratic cost function are R_e and Q_e . These weights are often set to the approximate values of the variance of the measurement noise $v(k)$ and process noise $w(k)$, respectively. The Kalman gain is proportional to Q_e/R_e and as such R_e and Q_e are often adjusted to obtain better state estimation. Sophisticated methods such as *Loop Transfer Recovery* can be employed for adjusting the Kalman weighting factors [44].

A diagram showing the set-membership robust control scheme is shown in Figure 23.

For our example the process noise $w(k)$ is negligible; the measurement noise $v(k)$ has a variance of 0.01 and mean of 0.0. When calculating the controller gain K we make use of the fact that the solution is invariant to the elements of the third column of Q above. The solution of the Riccati equation of (3.18) may be carried out with the simpler matrix

$$Q = \begin{bmatrix} 1 & 0 \\ 0 & 0 \end{bmatrix}.$$

Using the actual values of the plant the solution of (3.20) gives the LQR gain

$$K = [0.7886 \quad 0.6119]^T.$$

The scale factor V in the control equation is computed from the condition of the zero steady-state control error. For a value of k approaching infinity it holds that

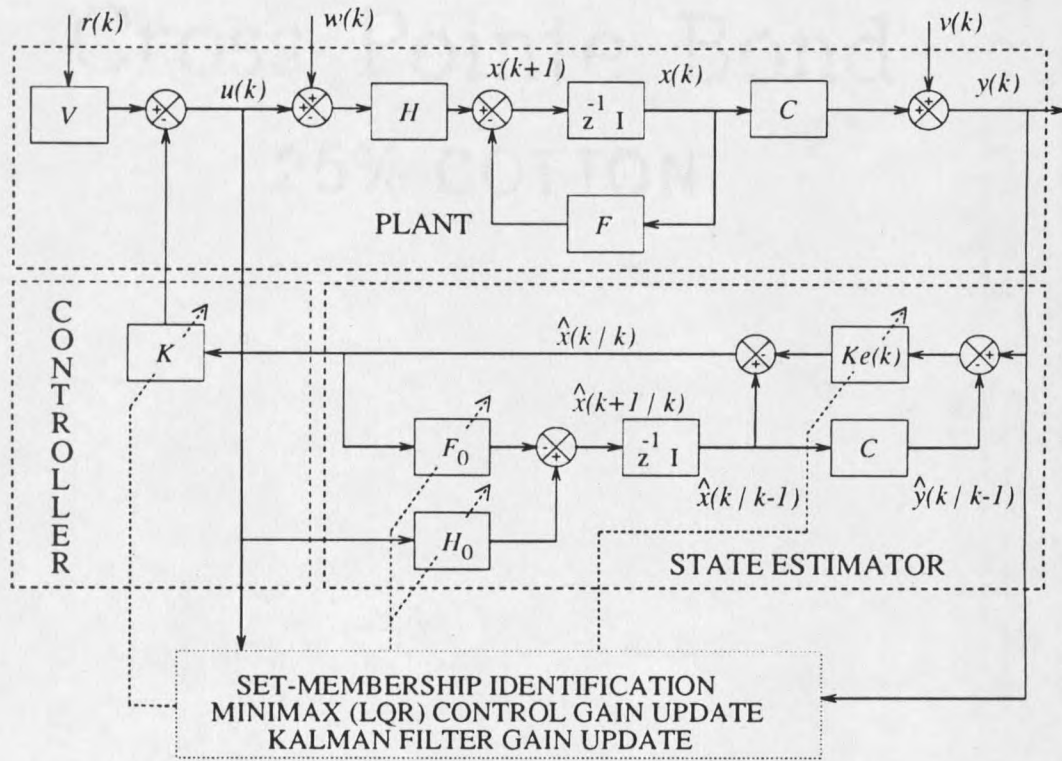


Figure 23. Set-membership adaptive control detailed block diagram.

parameter	lower	nominal	upper
$-a_1$	-2.0489	-1.4958	-0.9428
$-a_2$	-0.0451	0.4952	1.0355
b_1	0.2991	0.9610	1.6230
b_2	-0.0876	0.6156	1.3187

Table 7. Interval bounds on parameters of Example 1 using OVE algorithm.

$\mathbf{x}(k+1) = \mathbf{x}(k)$ and $x_1(k) = y(k) = r(k)$. Allowing $r(k)$ to take on the value of 1, the following set of equations can be solved for V and the steady-state value for $x_2(k)$. Let $Fcl = F - HK^T$ be the 2×2 closed-loop control matrix with elements $fcl_{1,1}$, $fcl_{1,2}$, $fcl_{2,1}$ and $fcl_{2,2}$, and let $H^T = [b_1 \ b_2]$. The solution to V and $x_2(k)$ in steady-state is given by

$$\begin{bmatrix} V \\ x_2(k) \end{bmatrix} = \begin{bmatrix} b_1 & fcl_{1,2} \\ b_2 & fcl_{2,2} - 1 \end{bmatrix}^{-1} \begin{bmatrix} 1 - fcl_{1,1} \\ -fcl_{2,1} \end{bmatrix}. \quad (4.39)$$

Using actual values of the plant we find that $V = 0.4826$ and $x_2(k) = -0.5000$. The initial starting value of \mathbf{x} for calculation of the final cost was taken as a random sample from the Kalman filter estimates of the plant states before the feedback loop was closed. The initial starting value of \mathbf{x} was also used in **Algorithm 3** for the worst-case gain calculation. In the first case, system identification was not used and actual parameter values of the plant in the Kalman filter were used for state-estimation. The initial starting value of the states was $\mathbf{x}(0) = [0.2325 \ 0.8409]$. The estimated cost using actual plant values is $J = 0.8118$. The bound on the noise sequence $v(k)$ is $v_{max} = 0.328229$ which was used in the ellipsoid bounding technique of Cheung, et al., referred to as the OVE algorithm. The input probing signal was adjusted to obtain a signal to noise ratio at the output of approximately 65 dB. Using the OVE algorithm we determined a bounding ellipsoid which had an associated bounding interval given in Table 7. After 9 iterations of **Algorithm 3** the LQR gain was found to be

$$K = [1.2852 \quad 1.0291]^T$$

and the worst-case LQR cost was $J = 2.5627$. To calculate V and the steady-state value of $x_2(k)$ we defined $F_{cl} \triangleq F_0 - H_0 K^T$ and $H_0 \triangleq [b_1 \ b_2]$, where F_0 and H_0 are the appropriate matrices using the nominal values given in Table 7. The solution to V and $x_2(k)$ in steady-state is given by (4.39) and the values are $V = 0.7749$ and $x_2(k) = -0.4955$. The results for this servo example can be seen in Figure 24.

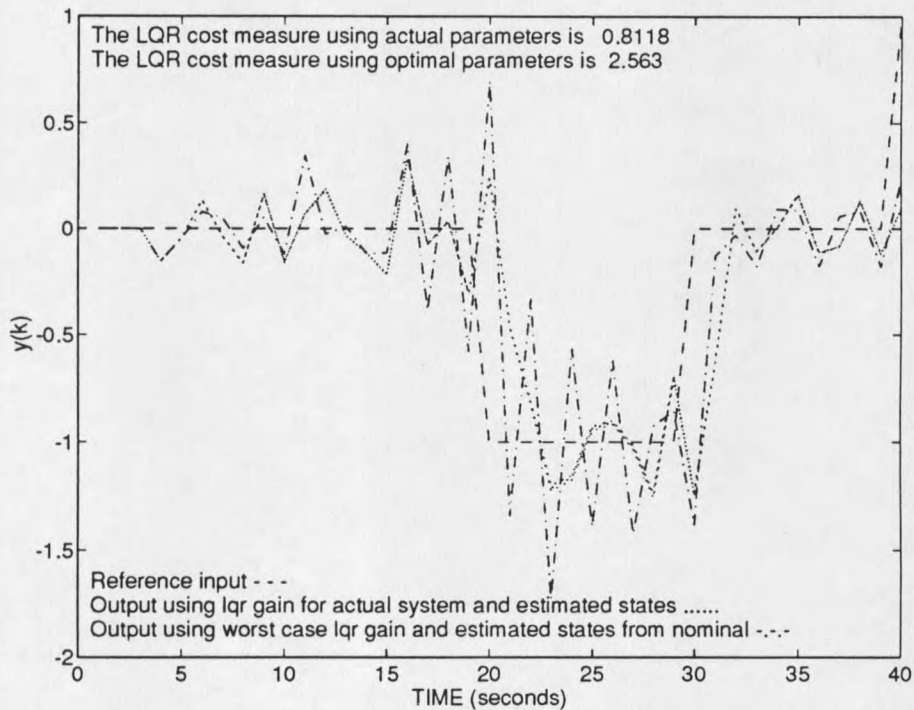


Figure 24. Servomechanism problem for standard LQG and set-membership control.

